CONTACT INFORMATION
Mining Records Curator
Arizona Geological Survey
416 W. Congress St., Suite 100
Tucson, Arizona 85701
602-771-1601
http://www.azgs.az.gov
inquiries@azgs.az.gov

The following file is part of the A. F. Budge Mining Ltd. Mining Collection

ACCESS STATEMENT

These digitized collections are accessible for purposes of education and research. We have indicated what we know about copyright and rights of privacy, publicity, or trademark. Due to the nature of archival collections, we are not always able to identify this information. We are eager to hear from any rights owners, so that we may obtain accurate information. Upon request, we will remove material from public view while we address a rights issue.

CONSTRAINTS STATEMENT

The Arizona Geological Survey does not claim to control all rights for all materials in its collection. These rights include, but are not limited to: copyright, privacy rights, and cultural protection rights. The User hereby assumes all responsibility for obtaining any rights to use the material in excess of "fair use."

The Survey makes no intellectual property claims to the products created by individual authors in the manuscript collections, except when the author deeded those rights to the Survey or when those authors were employed by the State of Arizona and created intellectual products as a function of their official duties. The Survey does maintain property rights to the physical and digital representations of the works.

QUALITY STATEMENT

The Arizona Geological Survey is not responsible for the accuracy of the records, information, or opinions that may be contained in the files. The Survey collects, catalogs, and archives data on mineral properties regardless of its views of the veracity or accuracy of those data.

REPORT
FOR THE RATTLER AND VICTOR CLAIMS
YAVAPAI COUNTY, ARIZONA

ENCLOSURES:

* REPORT
* EXHIBIT MAP OF LODE MINING CLAIMS
* GEOLOGY OF THE MORGAN BUTTE AREA
  YAVAPAI COUNTY, ARIZONA
  by David S. Gray
* ARIZONA ROAD MAP
* MORGAN BUTTE QUADRANGLE MAP
* GEOLOGICAL MAP OF THE MORGAN BUTTE AREA

REPORT ON THE RATTLER AND VICTOR CLAIMS

CLAIM NAMES: The Rattler Claims and the Victor Claims

DISTRICT: Blue Tank and Black Rock, Yavapai County, Arizona

MINERAL COMMODITIES: Gold, Silver and Uranium

LOCATION: T8N, R3W, G&SR B&M, Sections 4, 5, 8, 9, 10 and 15.
U. S. Geological Survey Topographic Map: Morgan Butte, Arizona, 7.5 Minute Series.

Elevation: 3200' to 4400'

Directions: Approximately 12 miles northeast of Wickenburg, Arizona, on the Constellation-Buckhorn road.

OWNERSHIP: Howard R. and/or Phyllis V. French
6407 W. Clouse Dr.
Phoenix, Arizona 85033
Phone: (602) 846-1942

PROPERTY DESCRIPTION AND STATUS

The claim group consists of 48 unpatented lode claims on Federal minerals. The surface ownership is Bureau of Land Management Trust Lands. The Rattler Group consists of: Rattler numbers 1 through 17, 21 through 45, 1E, 3E and 6E. The Victor Group consists of: Victor numbers 1, 2 and 3. Although the claim numbers form a discontinuous series, they are in reality a contiguous block and consist of the total property position. A map showing the block of claims is attached. All claim boundaries were established by Brunton compass and map survey. All monuments were in place September 26, 1981. Monuments consist of 2 x 2 inch stakes, 5 feet long.

HISTORY

During the period 1895-1927, this entire area was prospected and explored by numerous shafts, adits, and prospect pits. No record of shipments has been found for these particular claims; however, a number of shipments were made from some of the adjoining patented properties. In 1905, seven of the Rattler claims were owned by the Arizona Gold Mining Company, Wickenburg, Arizona. These claims were referred to in a pamphlet published in 1906 titled, "DESCRIPTION OF MINES AND PROSPECTS NEAR WICKENBURG," and quote: "The Arizona Gold Mining Co's property consists of 7 claims of about 20 acres each, situated in the Blue Tank and Black Rock districts, 12 miles northeast of Wickenburg, and is accessible by good traveled roads to and from Wickenburg, the stage passing over the property daily. It is also three miles from the Hassayampa river. Names of the claims are, towit: WALL STREET NO. 1, COPPER MARK, ALIDA, THELMA, DEXTER, LINNIE, and EVAL."

WORKINGS

Shafts:	10, with approximately 620 feet of depth
Adits:	19, with approximately 1690 feet of workings
Prospect pits:	Numerous

GEOLOGY

Refer to document: "GEOLOGY OF THE MORGAN BUTTE AREA, YAVAPAI COUNTY, ARIZONA," by David S. Gray.

MINERALOGY

Native gold with combined silver, limonite, quartz and calcite. Secondary copper minerals: cuprite, azurite, chrysocolla and malachite. Secondary uranium minerals are also present in some of the workings. Radioactive anomolies are in evidence on most of the claims.

SAMPLING

All samples were channel samples cut at the surface across the vein width (with a hammer and moil) and varying in width from six inches to six feet. The samples weighed from 10 to 50 lbs. and were placed in five-gallon plastic buckets for transport to the assay office, where they were crushed, split and assayed. Most of the tests were of the Atomic Absorption type with some 20% being Fire Assayed. The weighted average assay of 266 samples taken from these claims was .102 oz. of Au per ton, with an average sample width of 2.3 feet.

Several of the claims yielding better initial results were sampled more extensively:

Rattler #6 vein was scraped clear of debris with a bulldozer for a 300 foot length along the strike, exposing it to better advantage for sampling purposes. A total of 33 samples were taken at 8 foot intervals for 240 feet along this exposure, giving a weighted average of .151 oz. of Au per ton, with an average width of 5.02 feet. An additional 6 foot-deep trench was dug about the center of this exposure for 100 feet. Twenty-six additional 3 x 6 x 12 inch samples were taken along 26 feet of this oxidized boxwork and panned at the site. Native gold colors and wires were produced, indicating a possible ore shoot at this point.

Rattler #16 averaged .284 oz. of Au per ton over a 300 foot length with an average width of 2.13 feet.

Rattler #8D averaged .125 oz. of Au per ton over a 400 foot length and with an average width of 4.44 feet.

Rattler #8C averaged .107 oz. of Au per ton over a 300 foot length and an average width of 3.44 feet.

Rattler #28 averaged .317 oz. of Au per ton from five samples at the shaft and adit.

Obviously much more sampling needs to be done, preferably by core drilling, to delineate the depth of these deposits and possible tonnages available. All of the veins are well exposed and prospect roads have been dozed to most of them. There are five different target areas to concentrate on, with potential tonnages of over 100,000 tons. Water for development is accessible from four of the shafts on the property.

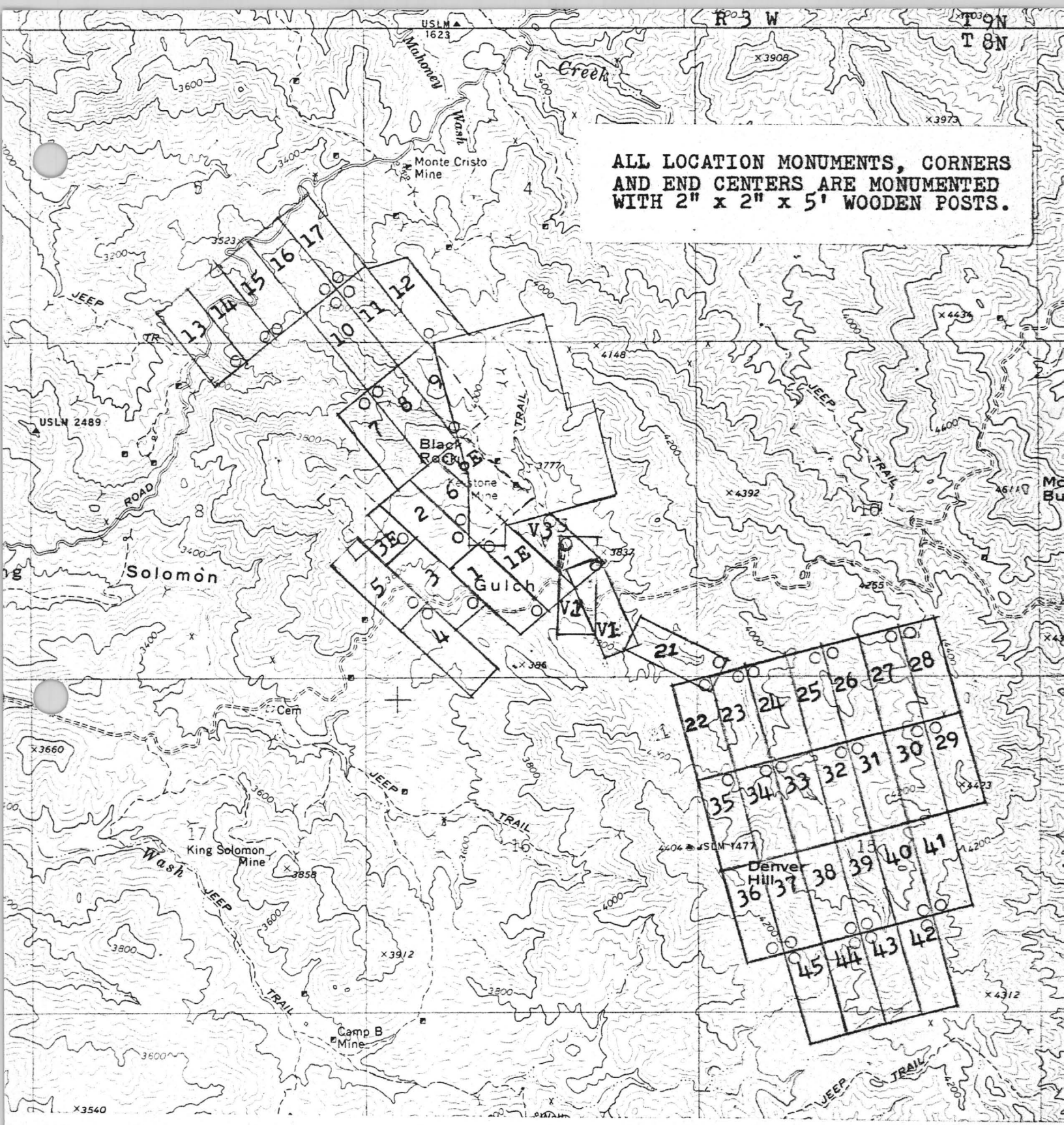

MN

14°

1"=2000'

EXHIBIT MAP
OF
LODE MINING CLAIMS
WITHIN
TOWNSHIP 8 NORTH, RANGE 3 WEST
YAVAPAI COUNTY ARIZONA
FOR
HOWARD R. FRENCH
6407 W Clouse Drive
Phoenix, Arizona 85033

RATTLER CLAIMS
1 - 17
1E, 3E, 6E

RATTLER CLAIMS
21 - 45

VICTOR CLAIMS
1 - 2 - 3

GEOLOGY OF THE MORGAN BUTTE AREA, YAVAPAI COUNTY, ARIZONA

A Thesis

Presented to

the Faculty of the Graduate School

Northern Arizona University

In Partial Fulfillment

for the Requirements for the Degree

Master of Science

---

by

David S. Gray

October 1982

GEOLOGY OF THE MORGAN BUTTE AREA, YAVAPAI COUNTY, ARIZONA

A Thesis in Geology

in Partial Fulfillment

of the Requirements for the Degree

Master of Science

---

by

David S. Gray

Approved:

Research Committee

Date: Oct. 8, 1982

ABSTRACT

Field and laboratory study of the geology in the Morgan Butte area, Yavapai County, Arizona, has revealed a complex Precambrian igneous and metamorphic history. No further earth history is evidenced until the late Tertiary, when faulting controlled emplacement of dikes of varying compositions and hydrothermal vein deposits.

Accumulation or emplacement of basites of an igneous origin, contemporaneous with the Yavapai Series, is the oldest known event. Before the metamorphism of the Yavapai Series, the basites were intruded extensively by a plutonic igneous rock of monzogranitic composition. Metamorphism of the two rock types to the lower amphibolite facies occurred, leaving some primary textures intact and creating a new mineral assemblage in the metabasites. Subsequent to the metamorphism, another plutonic episode, with intrusive bodies of dioritic to granitic composition, culminated in the emplacement of a large batholith of biotite granite. The intrusion of the batholith, with associated injection of granitic dikes and pegmatites, has created a migmatite in the metamorphic terrane.

The Tertiary record begins in the Miocene (?) with the onset of Basin and Range tectonics. Emplacement of rhyolite porphyry and mafic dikes, hydrothermal vein deposits and normal faulting were strongly controlled by a northwest structural fabric associated with the nearby Castle Hot Springs tectovolcanic depression. The hydrothermal vein deposits appear to have been emplaced at a depth typical of the epithermal zone. Several characteristics of the epithermal and deeper zones of emplacement coexist, and suggest a xenothermal origin for the vein deposits.

ACKNOWLEDGEMENTS

I would like to thank Gordon Swann of the Geological Survey in Flagstaff for his indispensable aid. Without his resources, this project would have been considerably more trying.

For a taste as close to the Old West as one can get these days, I thank Lou and Leslie Townshend and the rest of the Red Bluff crew. Without their hospitality and demeanor, the field work would have been far more lonely and unexciting. I would like to thank Howard French of Phoenix, Arizona, for a friendly face, rather than a gunbarrel, and his appreciation of my work out there.

Appreciation also goes to the late Plateau Resources, Ltd., for some materials at the start of this project.

For their excellent company in the field, I express gratitude to the following: Keith Shallcross, who made sure the snakes and scorpions will never be the same; Walter G. James III, for lugging that skull I don't know how far, and his excellent cooking in the field; and Bert Fowle. Bert and I, while playing army for years as kids, never thought that one day we would be dodging real bullets. I also express gratitude to my parents for their neverending encouragement and support.

And last but not least, I give thanks to Crazy Bill Latta, a certain shotgun toting gentleman, for making me think twice about some of the things I do in life.

TABLE OF CONTENTS

TABLE OF CONTENTS (Continued) Page

TABLE OF CONTENTS (Continued) Page

LIST OF ILLUSTRATIONS

LIST OF ILLUSTRATIONS (Continued) Page

LIST OF ILLUSTRATIONS (Continued)

Page

Chapter 1

INTRODUCTION

Location and Accessibility

The Morgan Butte area (Plate 1), located in the northern Wickenburg Mountains, encompasses approximately 31 square kilometers (12 sq. mi.) and is located between 17 and 24 kilometers (11 and 15 mi.) northeast of Wickenburg, Arizona (Figure 1). Accessibility is excellent on the county maintained Constellation and Buckhorn roads to the western and southern portions of the area. The Constellation road leaves downtown Wickenburg on the east side of the Hassayampa River and branches into the Buckhorn road about 1.6 kilometers (1 mi.) outside the southwestern corner of the study area. The northern, eastern and central portions are accessible only by foot or private roads. Most of the area falls under the jurisdiction of private mining claims and permission is required for access.

Physiography

Elevation above sea level in the study area ranges from 850 meters to 1405 meters (2800 to 4611 ft.) on Morgan Butte. The area is intricately and sharply dissected by a rough northwesterly drainage into the Hassayampa River. In addition, there is a weaker pattern of northeastern drainage generally feeding the more prominent northwest drainage.

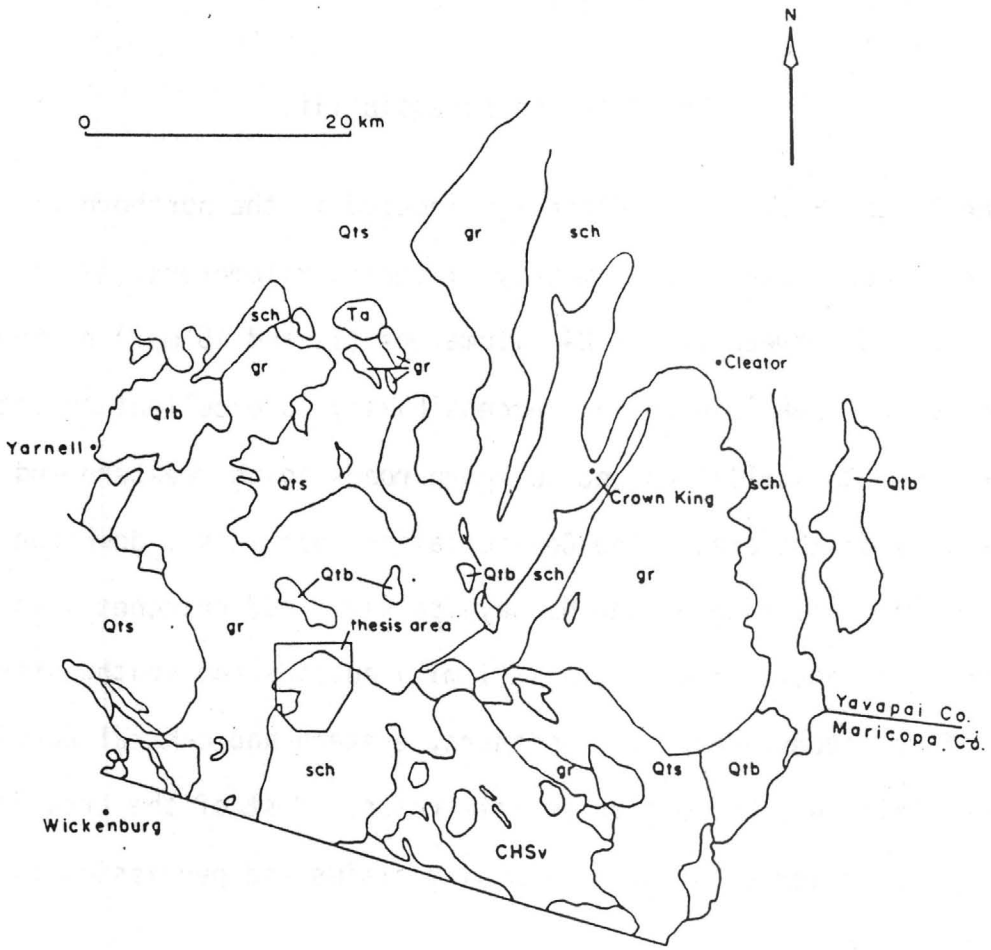

Figure 1. Map of South Central Yavapai County Showing the Location of the Study Area and Surrounding Geology. Adapted From Map 3-10, Geologic Map of Yavapai County, Arizona, Bureau of Geology and Mineral Technology, Tucson. CHSv = Castle Hot Springs Volcanics, gr = granite, sch = schist, Qtb = Quaternary basalts, Qts = Quaternary sands, silts and gravels.

Traversing the study area in a northeast direction, the relief becomes more pronounced; the valleys become narrower and deeper and the ridges longer and more pronounced.

Climate and Vegetation

The area is in the Upper Sonoran Zone. The summers are extremely hot with temperatures well over one hundred degrees Fahrenheit, while the winters are pleasantly mild. Average annual rainfall is less than ten inches and most of this occurs during the late winter months. The climate is nearly always very dry; during the hot months a dry, hot wind often blows from the lower basins to the southwest.

The vegetation is a typical assemblage of Upper Sonoran desert plants. Saguaro, barrel, fishhook, prickly pear, and several varieties of cholla cactus are common. Mesquite, palo verde, and catclaw are also abundant. On some of the higher northfacing slopes, manzanita can be quite thick but does not impede progress on foot.

Regional Geologic Setting

The Wickenburg Mountains, the Buckhorn Mountains and the more extensive Bradshaw Mountains to the north of the study area are located in a belt of dominantly Precambrian rocks outcropping northwest-southeast through central Arizona. This belt is bounded tectonically on the northeast by the Colorado Plateau and merges into the Basin and Range Province to the southwest. Included in this Precambrian belt are a variety of rock types of several orogenic episodes as well as Tertiary volcanic rocks.

The Yavapai and Pinal Series as well as the Vishnu Series in the Grand Canyon are overlain in some localities by unmetamorphosed younger Precambrian sedimentary and volcanic rocks. In the Wickenburg and Bradshaw Mountains this sedimentary cover is missing and the Yavapai Series is exposed in outcrops up to 2133 meters (7000 ft.) in elevation. The Yavapai Series as described in the Cleator area is typical of a greenstone belt (Vrba, 1980).

Southeast of the Morgan Butte area is a region approximately 160 square kilometers (62 sq. mi.) in extent, covered by Tertiary basaltic, rhyolitic and latitic tuffs and lavas known as the Castle Hot Springs volcanics (Ward, 1977). The bulk of these volcanics is between 6 and 14 kilometers from the study area. Over 400 meters (1300 ft.) of the tuffs and lavas fill a northwest trending volcanotectonic depression. The southwest boundary of this graben passes the northeast corner of the Morgan Butte area. There are several isolated buttes of basaltic lavas and agglomerates only 1.6 to 4.8 kilometers (1 to 3 mi.) north of the mapped area. These are lower in elevation than the Precambrian rocks of the Morgan Butte area immediately south and west of the graben.

Previous Work

The first significant work in this area was a regional reconnaissance of the Bradshaw Mountains by T. A. Jaggar, Jr. and C. Palache. The results were published in the U.S.G.S. Atlas Folio 126 in 1905. They covered an area of 2550 square kilometers (986 sq. mi.) and provided general descriptions of many different and complex areas. In 1922, E. S. Bastin studied the vein mineralogies in the Monte Cristo Mine to shed light on the nickel-cobalt deposits of Cobalt, Ontario.

In 1926, Waldemar Lindgren conducted a reconnaissance study of the ore deposits in the Bradshaw Quadrangle. The Morgan Butte area is in the Congress Quadrangle but is directly adjacent to the west of the Castle Creek District described by Lindgren.

Charles Anderson (1951) covered the Morgan Butte area in another regional overview when he correlated the Vishnu, Pinal and Yavapai Series. His description of the Yavapai Series centered around Jerome, 61 kilometers to the north. Richard Johns (1952) conducted a detailed study of the White Picacho pegmatites located about 11 kilometers (7 mi.) to the south. The study concerns the pegmatites and contains only a brief description of metamorphic rocks of the Yavapai Series. Many of these metamorphic rocks are not represented in the Morgan Butte area.

Michael Ward (1977) studied the Castle Hot Springs volcanics to the southeast and only briefly describes the Precambrian bedrock. A detailed study of the lithium minerals in the White Picacho pegmatites was conducted by David London (1979), but again only a brief description of the Precambrian metamorphic and plutonic rocks is given. Simple, tourmaline bearing pegmatites are abundant in the Morgan Butte area but no complex pegmatites were observed by the author.

No previous work has been done in this area that mapped the Precambrian bedrock in detail.

Purpose and Methods

There are three main objectives to this investigation: 1) to present a detailed petrologic study of the various lithologies of Precambrian age, 2) to provide a detailed geologic map of the area at a scale

of 1:12,000 and 3) to fit the mineral deposits into the geologic chronology.

These goals were met by the use of standard field mapping techniques and laboratory petrographic study. Aerial photos were of use in mapping the major vein deposits. Two hundred and twenty rock fabric measurements and 142 samples were obtained in the field. Ninety-seven thin sections were made by the author from which 38 point counts were taken. The point counts were converted to oxide weight percents by the technique outlined in Appendix I to produce simulated chemical analyses of the metamorphic rocks. Real mineral analysis from geologically similar environments were used as a standard. This technique is applicable only to phaneritic rocks from which point counts can be made. Fortunately, phaneritic rocks are the rule in the Morgan Butte area. Plagioclase compositions were determined by the Michel-Levy method (Moorehouse, 1959).

Chapter 2

PRECAMBRIAN METAMORPHIC ROCKS

Introduction

Two types of metamorphic rocks are present in the Morgan Butte area. A granitic gneiss is the most abundant type and contains abundant inclusions of amphibolite throughout its exposure area (Figure 2). The amphibolite inclusions tend to increase in abundance towards the larger bodies of amphibolite; however, this is not a trend without exception. Three out of four of these are adjacent to postmetamorphic granitic inclusions as well as contained in the granitic gneiss (Plate 1). These amphibolite bodies exhibit a variety of shapes that have been modified by the postmetamorphic Precambrian intrusions. The dimensions of these amphibolite bodies after these events are on the order of hundreds of meters to over one kilometer in maximum dimension.

Upon intrusion of a postmetamorphic biotite granite of batholithic proportions, both the amphibolites and granitic gneisses were injected extensively by crosscutting granitic dikes, pegmatites and medium grained alaskitic intrusive bodies. The metamorphic terrane is now, in essence, a migmatized gneiss.

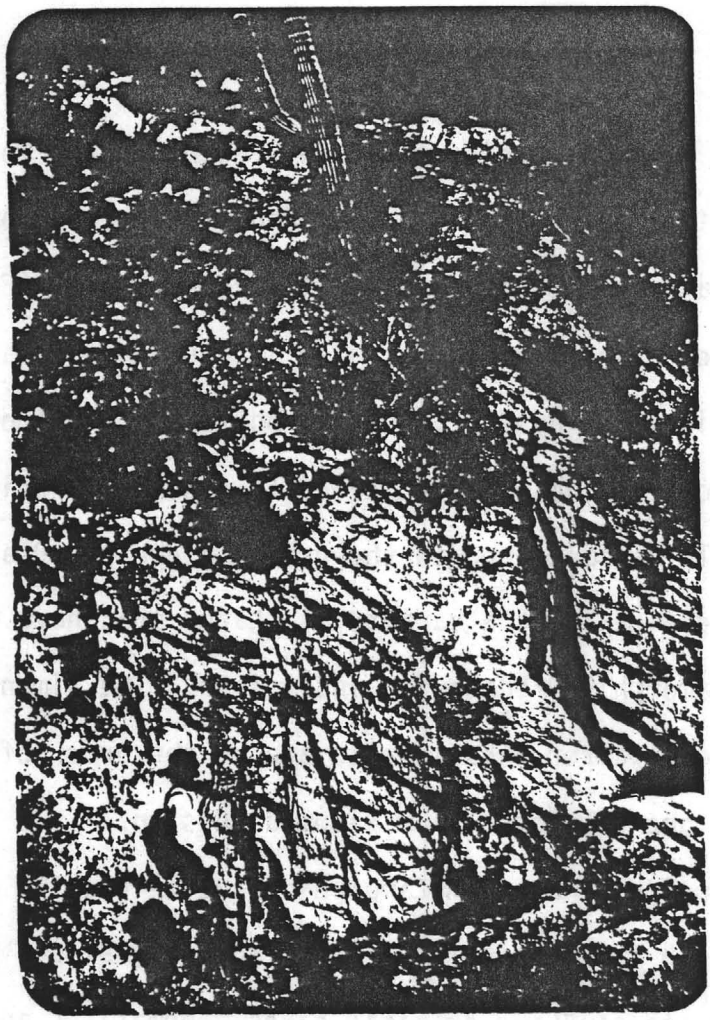

Figure 2. Photograph of Amphibolite Inclusions in Granitic Gneiss.

Amphibolite

Metamorphism

Equilibrium assemblages in the amphibolites, as outlined by Miyashiro (1973), indicate that it reached a grade of metamorphism equivalent to the lower amphibolite facies. The amphibolite contains 45-70% blue-green hornblende and 30-50% andesine. Varying amounts of biotite and quartz are usually present. Biotite in excess of hornblende can occur, but is rare and is commonly absent. Biotite is usually included in a crystal aggregate with hornblende, but can also be found as separate grains. Quartz is also commonly absent and rarely exceeds 20% of the rock.

Care must be taken to distinguish quartz derived from the amphibolite and quartz injected from intrusion of silicic plutonic rocks. Quartz in veinlets with microcline indicates it was a later addition to the rock. As the content of metamorphic quartz increases, the amphibolite grades into a hornblende-plagioclase gneiss.

Epidote in small amounts (2-5%) is commonly present. Some of the epidote is from a later retrograde event and is not representative of the equilibrium assemblage attained in the lower amphibolite facies. Some epidote is concordant with the metamorphic foliation and banding (S_1), suggesting it is part of the equilibrium assemblage. Magnetite, sphene, sulfides and apatite are common accessories. That the assemblage of hornblende-andesine-biotite-quartz reached equilibrium in the lower amphibolite facies is evidenced by the following criteria outlined by Miyashiro (1973):

1. Blue-green hornblende is stable into the lower amphibolite facies.
2. The blue-green hornblende grains commonly exhibit triple grain boundary junctions with each other indicating equilibrium (Figure 3).
3. Plagioclase of An_{30} in equilibrium with epidote is the boundary between the epidote-amphibolite facies and the amphibolite facies. Plagioclase in the Morgan Butte amphibolites average An_{39}. This shows the boundary to the amphibolite facies was passed.

The presence of biotite and epidote does not contradict this assemblage. Biotite is stable from low greenschist to granulite facies and epidote gradually decreases in abundance with rising temperature to add calcium to the plagioclase. The equilibrium assemblage with appropriate tielines is plotted on an ACF diagram with the respective rock composition plots in Figure 4.

A retrograde metamorphic event occurred to alter the mineralogy and destroy some of the textures developed in the lower amphibolite facies. The retrogradation is not ubiquitous, however, and varies greatly from sample to sample. Some amphibolites are quite clean of any alteration products formed by the retrograde event, whereas in others the hornblendes, biotites, and plagioclases are nearly completely gone.

Chlorite, often with anomalous blue interference colors, magnetite and more rarely, epidote, are alteration products of the hornblendes and biotites. Saussuritization of the andesine grains (Figure 5) is more prevalent than the chloritization of ferromagnesian minerals. Epidote is more common and rarely occurs in a radiating habit when the

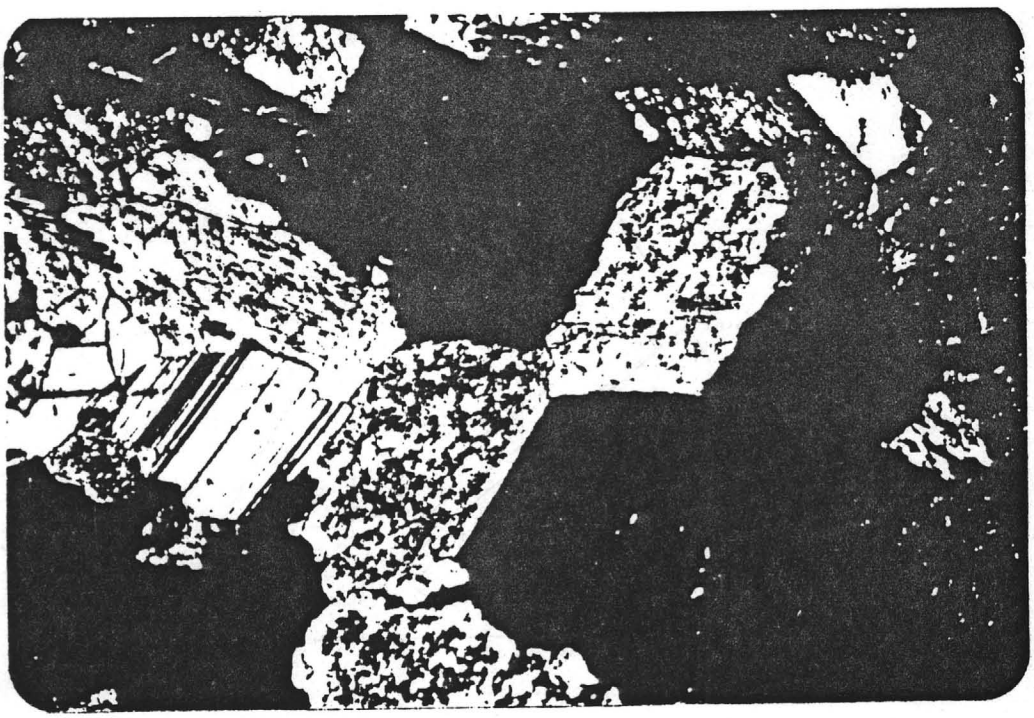

Figure 3. Photomicrograph of Triple Grain Boundary Junctions of Blue-Green Hornblende. 50x.

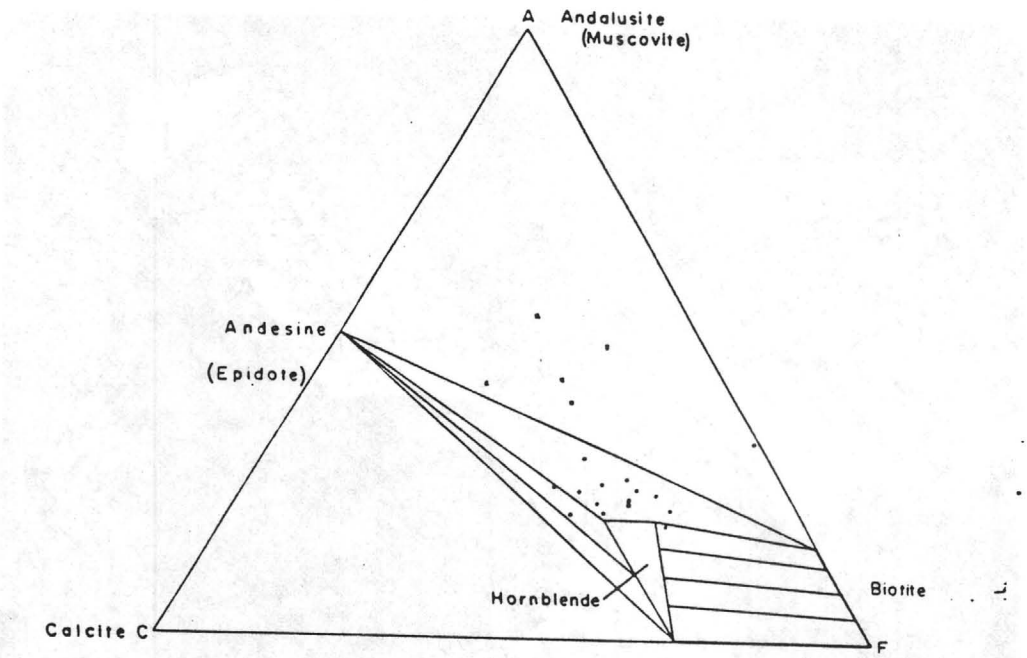

Figure 4. ACF Diagram (adapted from Miyashiro, 1973) Showing an Equilibrium Assemblage of Hornblende-Andesine-Biotite, and Quartz in the Lower Amphibolite Facies. Fifteen Amphibolite (·) and Five Granitic Gneiss (x) Compositions are Plotted for Comparison.

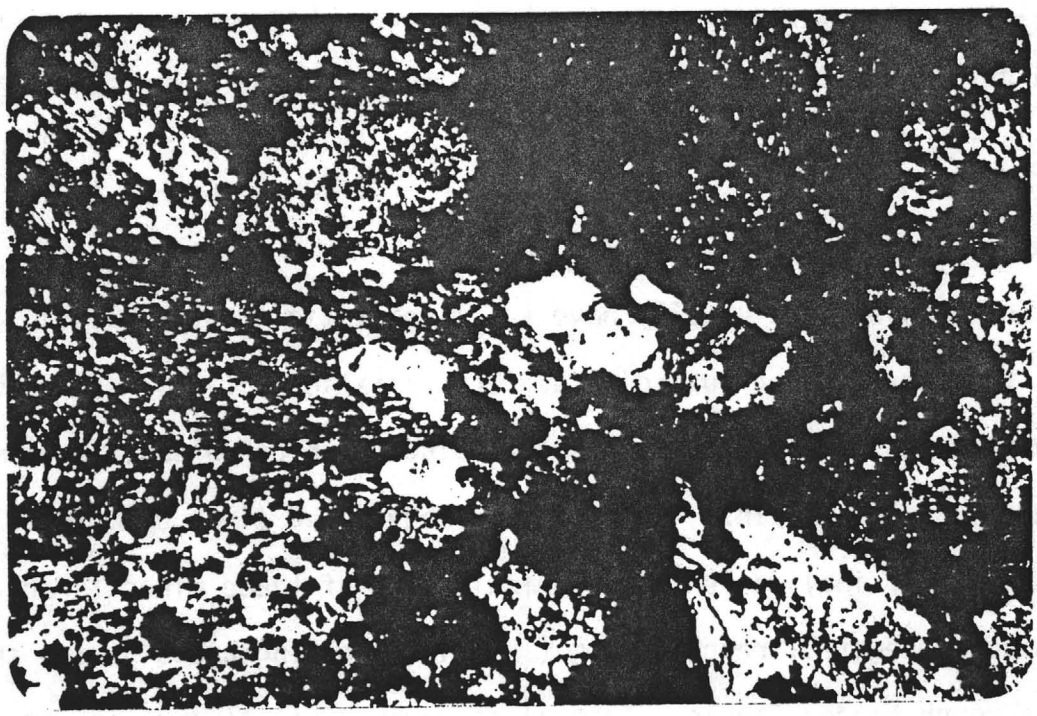

Figure 5. Photomicrograph of Altered Andesine. 50x.

plagioclases are heavily altered. Epidote coated joint surfaces are abundant. Epidote existed in both prograde and retrograde environments and the origin of each type cannot always be distinguished when both are present. The development of albite also accompanies the retrograde alteration, presumably from the breakdown of andesine. Albite commonly embays the altered plagioclase and hornblende. Hornblende is also commonly poikiloblastic to albite. Albite is not stable beyond the epidote-amphibolite facies.

Textures

The amphibolites usually have a nematoblastic to granoblastic texture, the latter being subordinate. The foliation (S_1) is defined by roughly elongate subhedral to anhedral blue-green hornblendes, .06mm to 1.4mm (.0024 to .055 in.) in length and andesine grains .08mm to 1.2mm (.0031 to .047 in.) in length. Commonly each of these minerals are in elongate aggregates, reaching 5mm (.197 in.) in length and giving the rock a rough banded fabric. This blastoporphyritic texture is more commonly shown by hornblende (Figure 6) than by plagioclase. In many of the amphibolites unaffected by the retrograde metamorphism, grain boundaries between the hornblendes are straight and meet in triple grain junctions (Figure 3).

When biotite is present the rock takes on a lepidoblastic foliation. Biotite usually occurs in small anhedral flakes .1mm to .8mm (.004 to .031 in.) in length and is concordant to the hornblende-plagioclase banding when it is present.

Granoblastic amphibolites with individual subhedral crystals of hornblende and andesine reaching lengths of 4mm (.157 in.) and 2.5mm (.098 in.) respectively, make up a small proportion of the amphibolites.

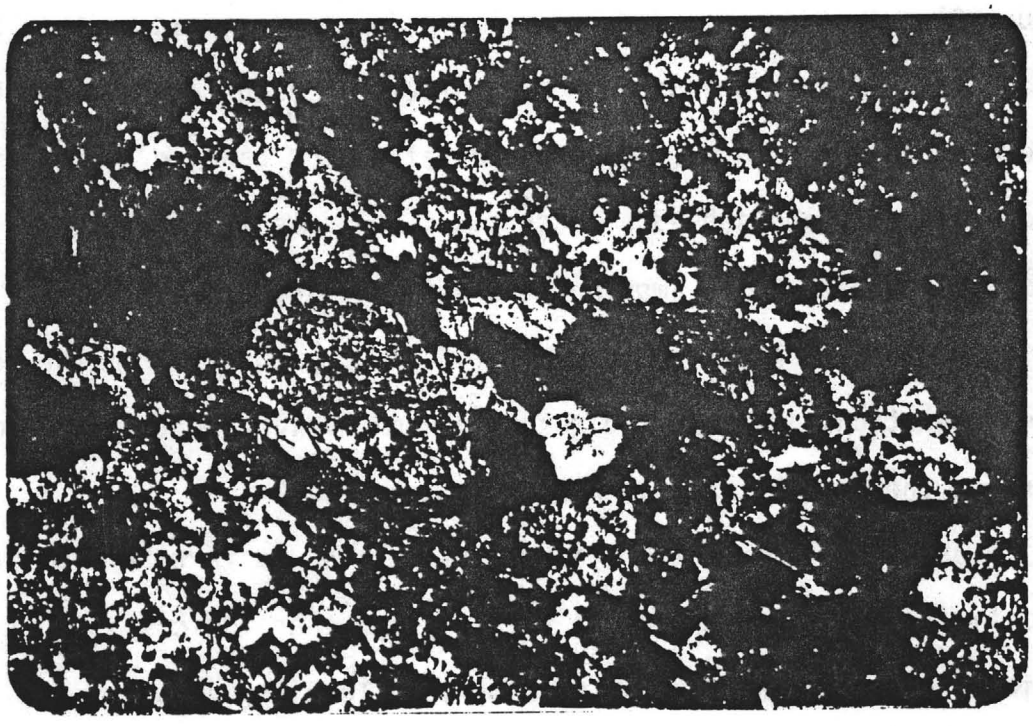

Figure 6. Photomicrograph of Blastoporphyritic Texture of Hornblende in Amphibolite. 50x.

A fabric typical of the amphibolites that underwent the retrograde metamorphism is a poikiloblastic hornblende with albite texture (Figure 7). The inclusions of albite and infrequent quartz are less than .1mm (.004 in.). Where the hornblendes have altered to chlorite there is an abundance of magnetite within and around the chlorite crystal boundaries (Figure 8). Iron is released upon alteration to form magnetite. Stubby and elongate epidote grains up to .7mm (.028 in.) in length occur both concordant to and across (Figure 9) foliation and banding. Subhedral to euhedral sphenes and subhedral magnetite, sulfides and apatites are scattered throughout the amphibolites as small accessory minerals.

Veinlets of calcite up to 1mm (.040 in.), probably from the retrograde alteration, and injected quartz and microcline up to dike proportions cut the amphibolites in many orientations.

Chlorite and propylitic alterations related to Tertiary hydrothermal activity are superimposed on the varying mineralogic states of the amphibolites where they are in proximity to Tertiary veins.

Origin of the Amphibolites

The amphibolites are considered by the author to be metabasites contemporaneous with the Yavapai Series. A metasedimentary origin is ruled out and a metabasite origin is favored on the basis of the following field relations and petrographic evidence:

1. The amphibolites are metaxenoliths of sizes ranging from thin, lenticular masses a meter (3 ft.) long and 15cm (5.9 in.) thick to large metamorphosed stoped blocks of basite. The metaxenoliths and blocks for the most part are contained and surrounded by a granitic

gneiss. The granitic gneiss is interpreted as a metagranite (below). In Precambrian rocks in surrounding areas (south and east) rocks like the granitic gneiss are not present whereas there are a variety of metamorphic rock types. The relative competency and melting temperature of a basite would make it the last type of country rock to be assimilated into a granitic magma intruding into an assemblage of different rock types. What type of metamorphic effects were caused by this premetamorphic intrusive event is unknown.

2. The amphibolites are horizonless. Aside from grain size differences, the amphibolites are homogenous. A uniform, monotonous medium grain size is the abundant type. There are no recognizable S_0 surfaces, either in the field or thin section.
3. Amphibolites of a metabasite origin abound in the Yavapai Series as well as the Pinal and Vishnu Series (Anderson, 1951).
4. The blastoporphyritic textures (Figure 6) are relict phenocrysts of both hornblende and plagioclase, the former being more abundant.
5. Sphene and magnetite are commonly associated together as an accessory crystal aggregate. The magnetite is probably titaniferous and with sphene suggests a magmatic origin rather than carbonaceous shale or shaley dolostone (Hyndman, 1972).

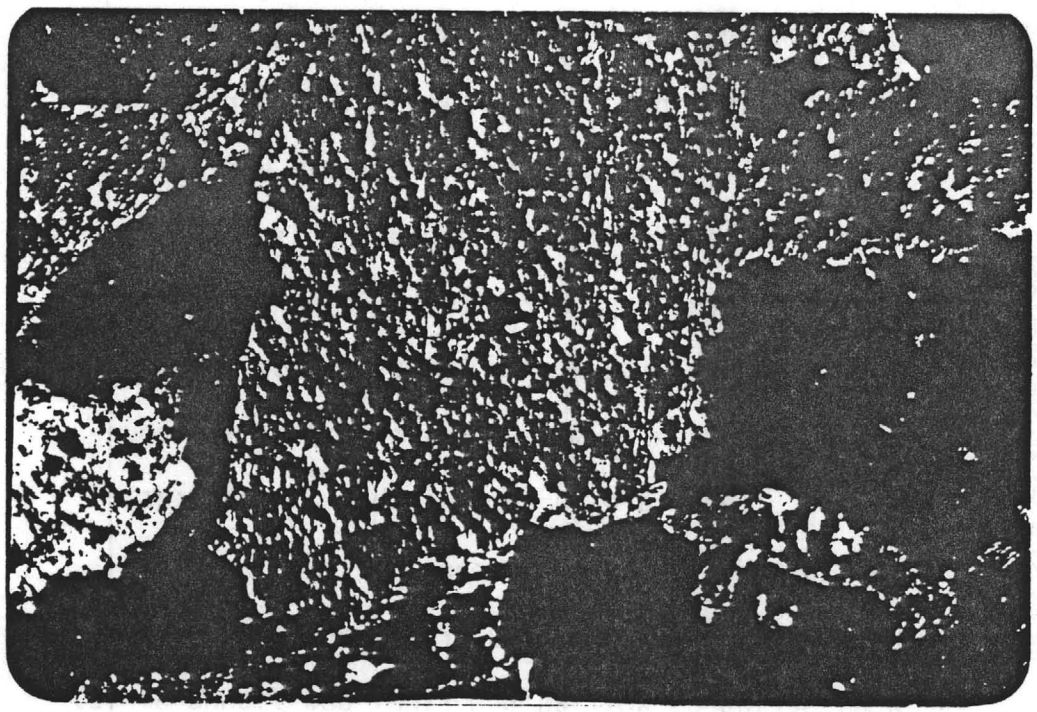

Figure 7. Photomicrograph of Poikiloblastic Texture of Hornblende with Albite and Quartz. 50x.

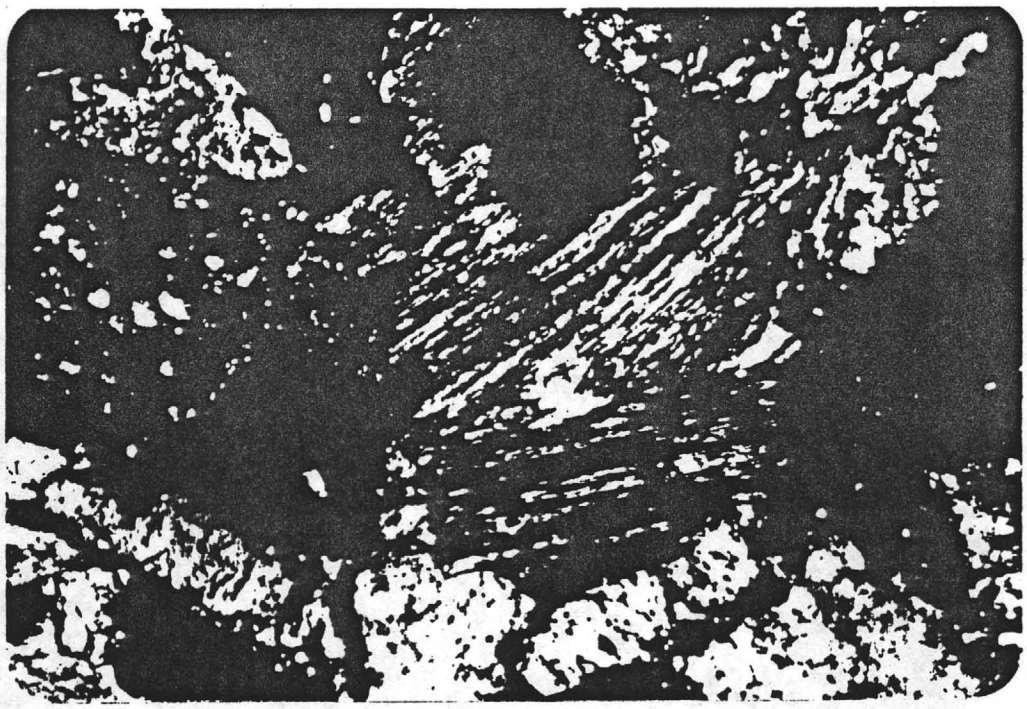

Figure 8. Photomicrograph of Mafic Mineral Altering to Chlorite with Associated Magnetite. 200x.

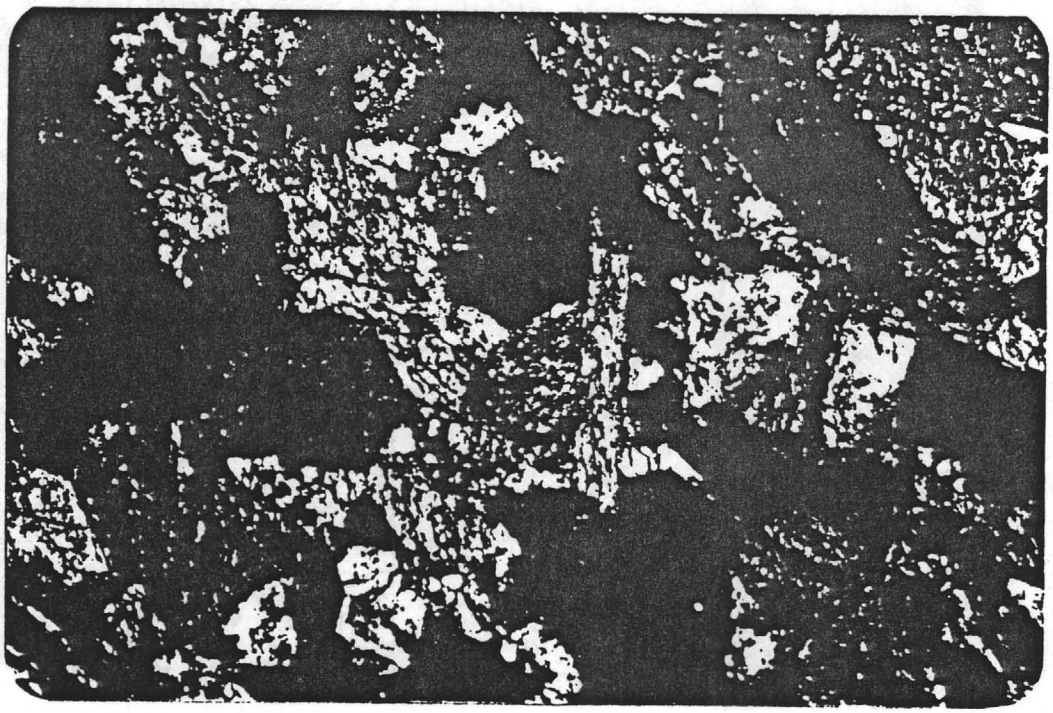

Figure 9. Photomicrograph of Epidote Discordant to Metamorphic Foliation. 50x.

6. A compositional plot on Miyashiro's (1973) ACF diagram shows that the Morgan Butte amphibolites fall in the basalt or andesite field (Figure 10).

Although the metabasite origin has been established, whether the amphibolite is a metavolcanic or a metaintrusive is unknown.

Origin of the Retrograde Metamorphism

The alteration caused by the retrograde metamorphic event is not ubiquitous. The local nature of the alteration indicate that the retrogradation is not regional. The extensive injection of the metamorphic rocks by hydrous magmas and fluids and the associated metasomatism is a probable cause for the retrograde metamorphism. Abundant pegmatitic and granitic dikes and veinlets originating from a postmetamorphic batholith of biotite granite shows that volatiles have played an important role in that stage of the intrusion.

Granitic Gneiss

Textures

The second and most abundant type of metamorphic rock in the area is a quartzofeldspathic gneiss. The gneiss is medium grained and contains biotite as the only mafic mineral. Plagioclase and microcline occur in roughly equal proportions. The gneiss is compositionally a monzogranite, if treated as an igneous rock (Streckeisen, 1976, Figure 11). The gneissic character is defined by quartz, plagioclase and microcline banded with up to 12% biotite (Figure 12). Andesine constitutes 30-35%, microcline 26-32%, and quartz 20-25% of the rock.

Strained anhedral quartz and subhedral plagioclase grains range from 1mm to 1.2mm (.040 to .047 in.) in length. Anhedral to subhedral

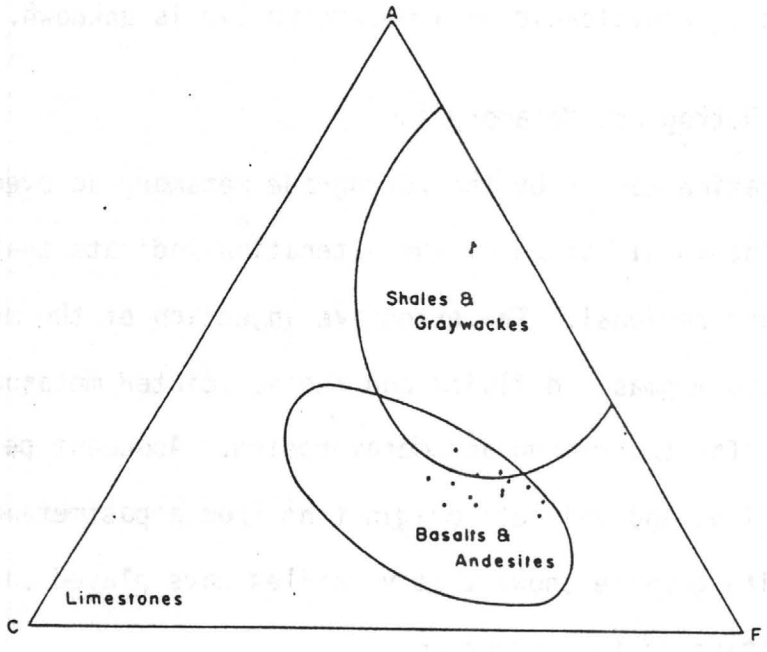

Figure 10. Fifteen Amphibolite Compositions Plotted Relative to the Compositional Fields of Some Rock Types on an ACF Diagram (Miyashiro, 1973).

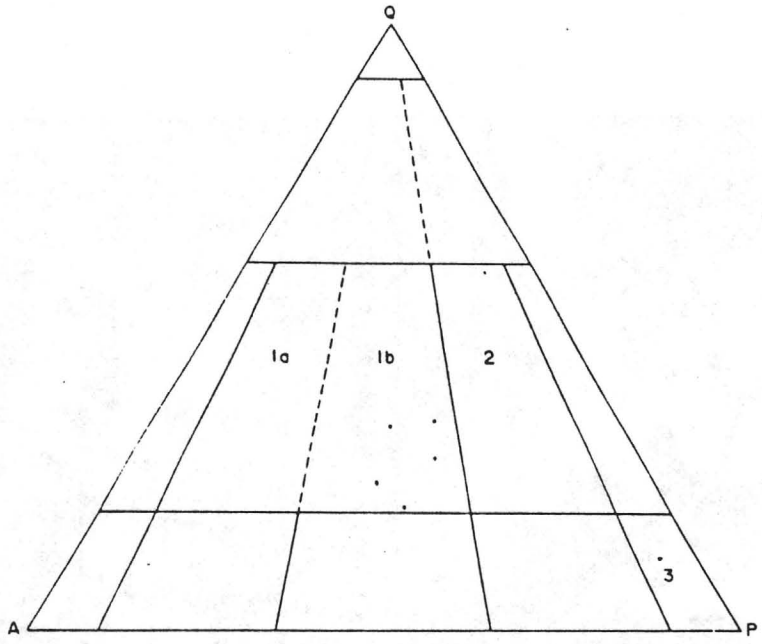

Figure 11. Five Granitic Gneiss Samples Plotted as an Igneous Rock on a QAPM Composition Diagram (Streckeisen, 1976). 1a = Syenogranite, 1b = Monzogranite, 2 = Granodiorite, 3 = Gabbro, Diorite, Anorthosite.

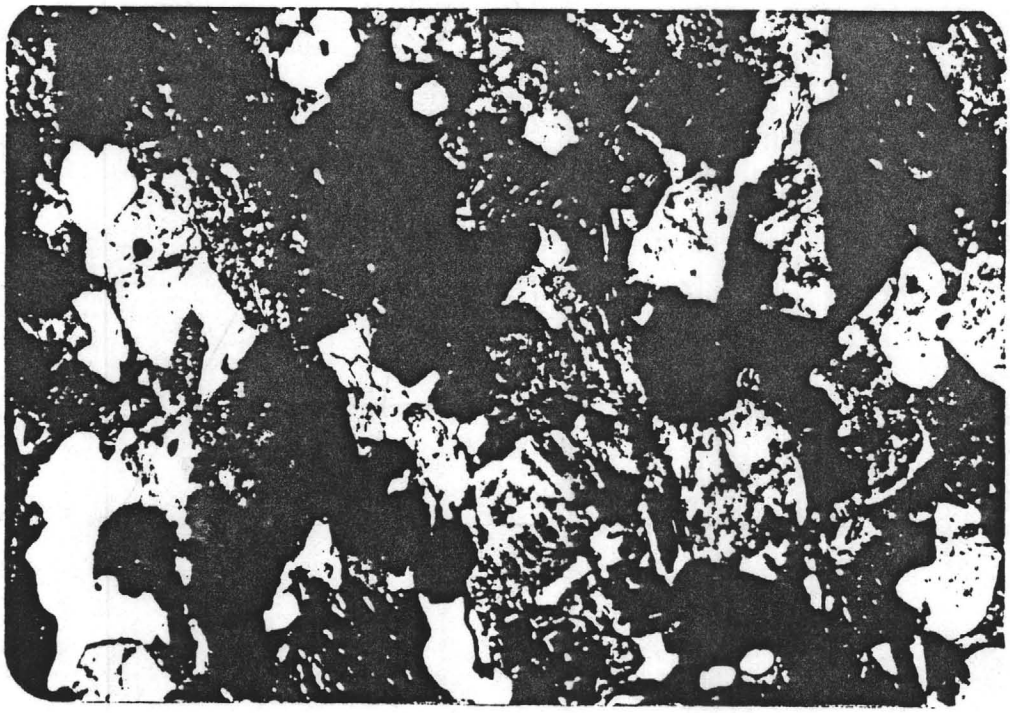

Figure 12. Photomicrograph of Granitic Gneiss Textures and Mineralogy. 50x.

microcline is also present as grains as small as 1mm (.004 in.). But microcline commonly reaches larger sizes as porphyroblasts up to 8mm (.315 in.) in length.

Anhedral biotite grains are commonly greater than 1mm (.040 in.) in maximum length and can be found in foliated aggregates up to 1.5cm (.591 in.) long. Subhedral epidote is common as an accessory mineral in some samples and absent in others. Epidote grains are typically less than 1mm (.040 in.) but rare crystals up to 2mm (.079 in.) were observed oriented across the foliation and banding. Small, round garnet grains (.1mm) are rare, but are present in the granitic gneiss. Other accessory minerals include small grains of muscovite, magnetite, zircon and apatite.

The granitic gneiss typically has a weak compositional banding parallel to a lepidoblastic foliation. Only rarely is the rock granoblastic with no foliation measureable.

Metamorphism

The granitic gneiss is undoubtedly metamorphosed to the same grade as the amphibolites. Although the mineralogic changes of an orthogneiss are less sensitive to changes in the pressure-temperature environment than a metabasite, the intimate association the two rocks have can lead to no other conclusion. The mineral assemblage shown in Figure 13 does not contradict a grade in the lower amphibolite facies. Although plagioclase compositions, when the grains are well twinned, average An_{33} (andesine), which is less than the andesine (An_{39}) in the amphibolites, it is probably due to the lesser amounts of calcium in a rock of granitic composition. Epidote and garnet are both stable in the lower amphibolite facies at medium pressure.

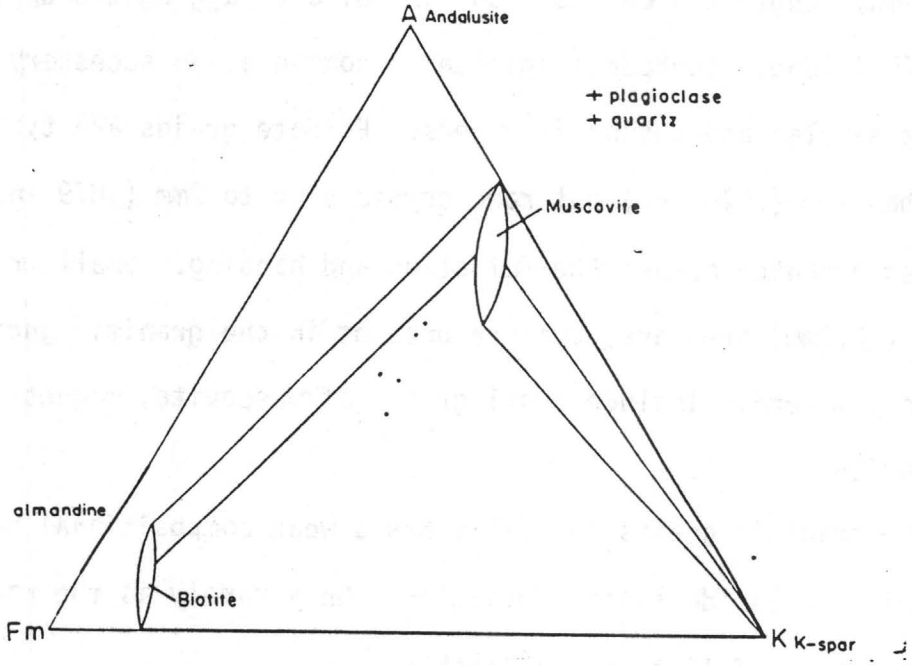

Figure 13. AKFm Diagram (Hyndman, 1972) Showing a Mineral Assemblage of Microcline-Plagioclase-Quartz-Biotite-Muscovite in the Granitic Gneiss in the Lower Amphibolite Facies and Five Compositional Plots.

The granitic gneiss has undergone retrograde metamorphism similar to the amphibolites. Chloritized biotite flakes with associated magnetite grains are common. Andesine grains are very commonly sericitized and less commonly saussuritized. As with the amphibolites, the retrograde metamorphism is not ubiquitous. Granitic gneiss samples quite clean of alteration are as abundant as samples with the biotites and plagioclases heavily altered. Microcline grains are rarely altered to sericite.

Origin of Granitic Gneiss

A plutonic parent rock for the granitic gneiss is evidenced by the following field and petrographic characteristics:

1. The homogeneous and medium grained texture over tens of square kilometers suggests the parent rock was also homogeneous.
2. A small percentage of the total bulk of the rock exhibits a striking blastoporphyritic texture (Figure 14) of microcline crystals up to 2cm (.787 in.) in length. This texture, interpreted as relict phenocrysts, is present in several parts of the field area and is particularly well developed several kilometers southwest of the area.
3. The rock is compositionally equivalent to a monzogranite (Figure 11). The mineralogy is essentially that of granite because there is little driving force for mineral change at this grade of metamorphism. Only the texture has been changed.

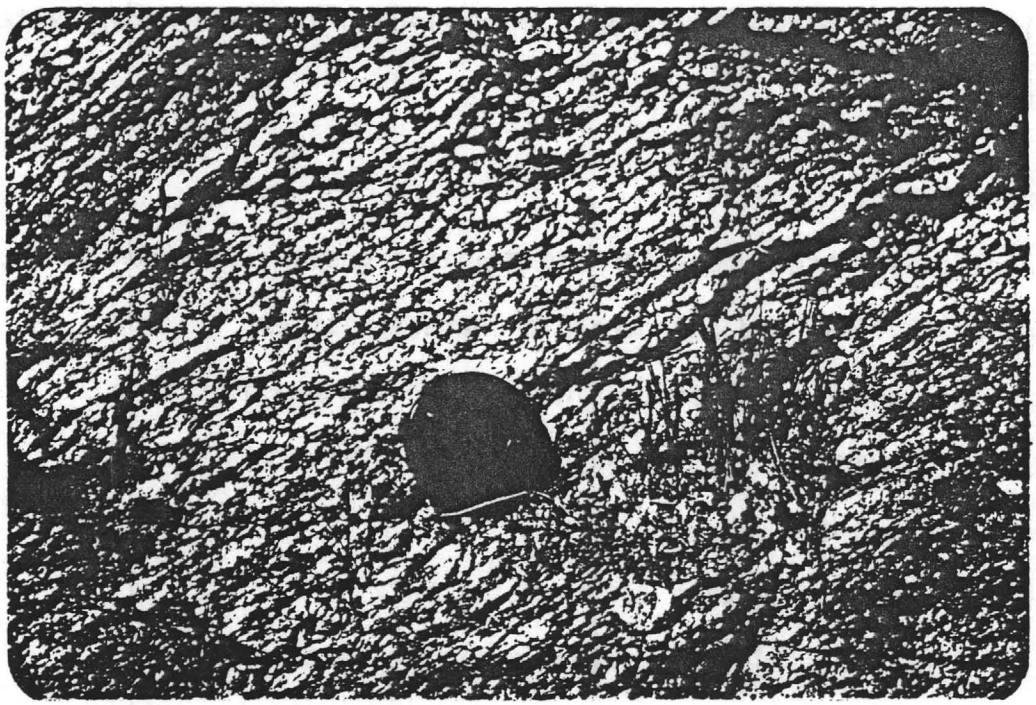

Figure 14. Photograph Showing Blastoporphyritic Texture of Microcline in the Granitic Gneiss.

4. The close association of the amphibolites and the granitic gneiss suggest a premetamorphic plutonic/country rock relationship. The amphibolite inclusions in the granitic gneiss cover a range of sizes from thin lenses (Figure 2) on the outcrop scale to blocks many kilometers in dimension. The metabasite inclusions are invariably concordant to the regional foliation developed in both the granitic gneiss and the amphibolites. A metasedimentary origin for the gneiss would have to take into account the inclusions of metabasite. Rare mica-rich lenticular inclusions, as shown in Figure 15, are possibly partially assimilated (and metamorphosed) xenoliths of a different texture and composition.

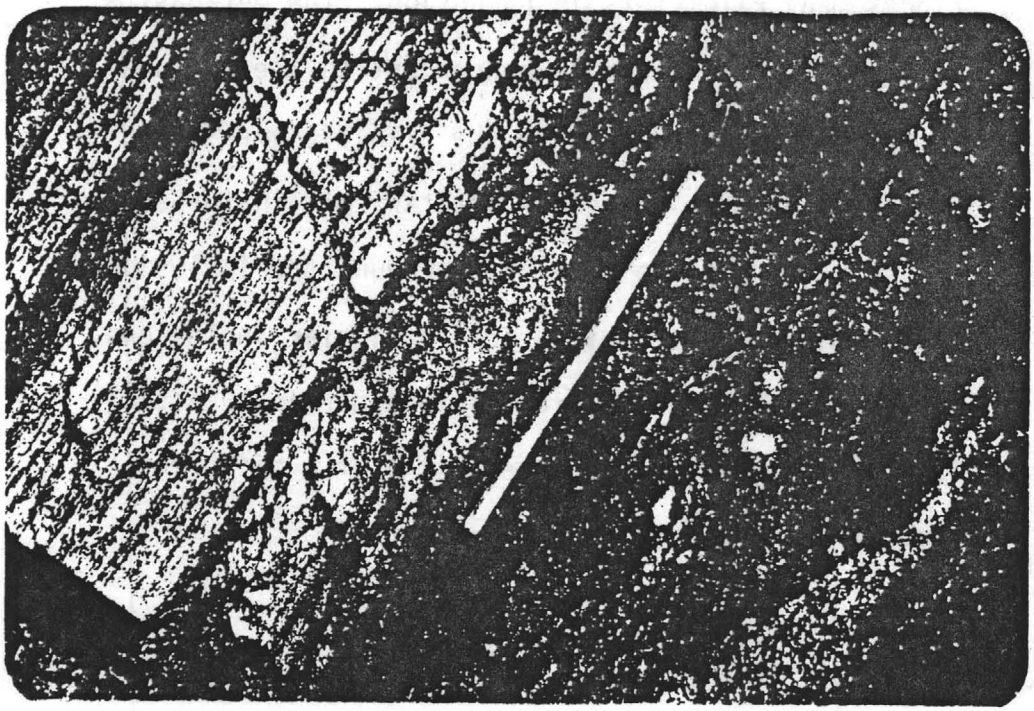

Figure 15. Photograph Showing Mica-rich Lenticular Inclusions in the Granitic Gneiss.

Chapter 3

PRECAMBRIAN PLUTONIC ROCKS

Introduction

Exposed in the Morgan Butte area are several varieties of igneous plutonic rocks. Lithologies range from diorites to several types of granitic rocks. The igneous plutons range from small irregularly round bodies (.75 to 1.5km) to one of batholithic proportions; and intrude the granitic gneiss and amphibolites. The smaller plutons are exposed in the southern part of the area and the batholithic contact is in the northern part. Two small dikes of hornblende diorite occur in the northeast corner of the Red Bluff mine properties.

Hornblende Diorite

Hornblende diorite is exposed as a small irregularly round pluton approximately one half to three quarters of a kilometer (.3 to .5 mi.) in diameter. The exposure is in the north fork of King Solomon Gulch, where it is partially covered by sands and gravels in the creek bed and by vegetation on the adjacent hills.

The hornblende diorite has a medium grained hypidiomorphic granular texture, defined by 35 to 40% hornblende and 35 to 55% plagioclase feldspar (Figure 16). A QAPM compositional plot according to Streckeisen (1976) is shown in Figure 17. Note that the absence of alkali feldspars causes the plots to be on the diorite edge of the diagram. Textural evidence where an epidote vein does not cut quartz indicates that the

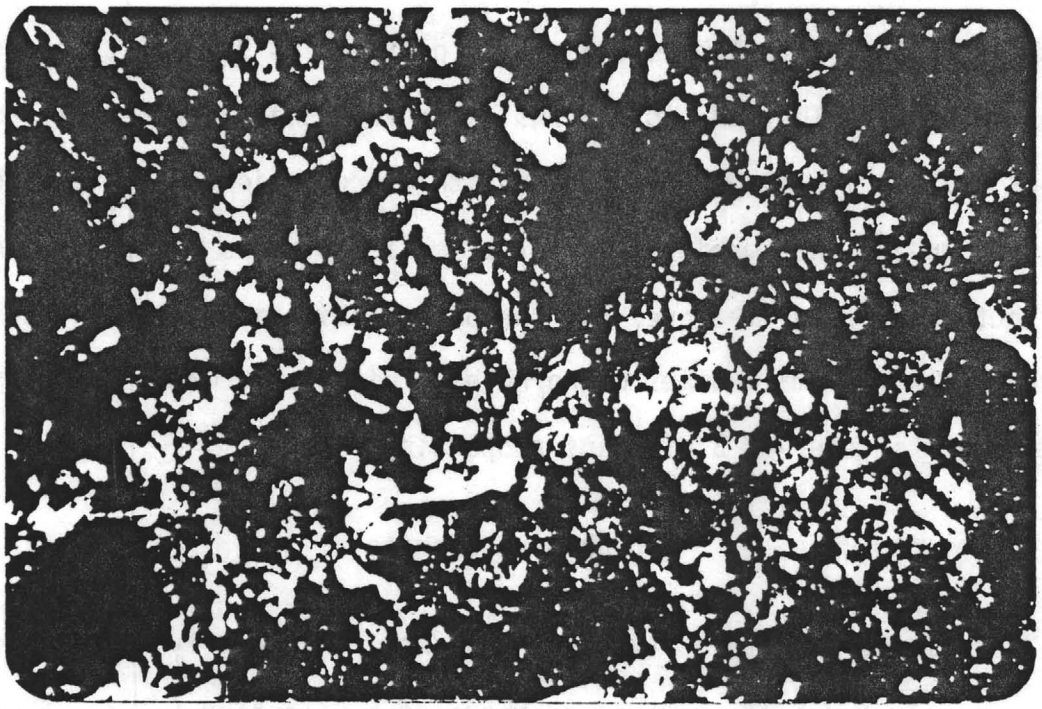

Figure 16. Photomicrograph of Hornblende Diorite Textures and Mineralogy. 50x.

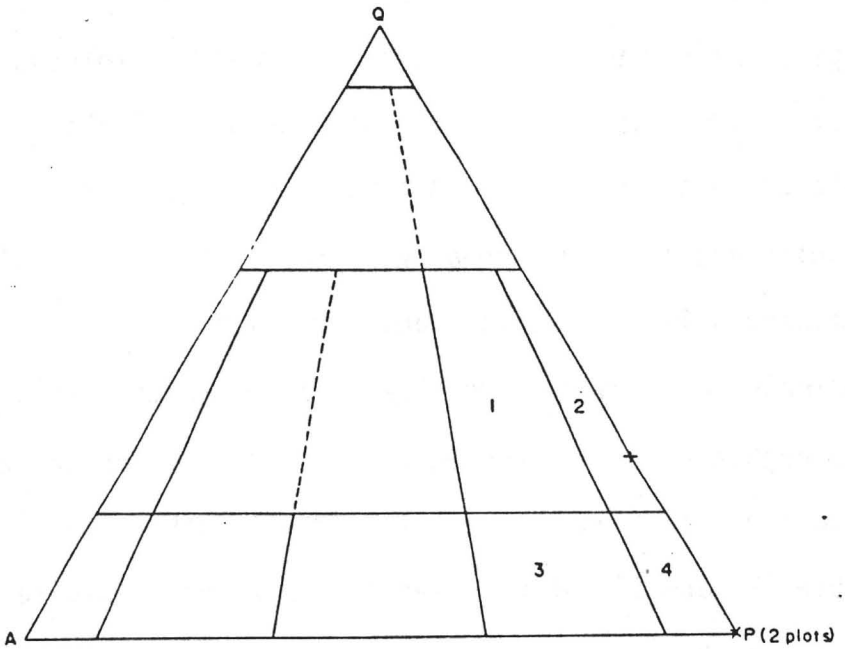

Figure 17. QAPM Compositional Plot (Streckeisen, 1976) of Three Hornblende Diorite Samples. 1 = Granodiorite, 2 = Quartz Diorite, 3 = Monzodiorite, 4 = Diorite, Gabbro.

quartz is a later addition, probably from injection of granitic material and alteration of the primary igneous minerals.

Hornblende crystals range from .1mm (.004 in.) to a typical 1.5mm (.059 in.) in length and are common in aggregates up to 6mm (.236 in.). Well twinned plagioclase grains reach 3mm (.118 in.) in length but usually average 1.5mm (.059 in.). Grains with poorly developed twinning are as small as .2mm (.008 in.). The unaltered plagioclase average 38% in anorthite content (andesine). Altered plagioclase grains where the twinning angles are still measureable, average 28% in anorthite content. Accessory minerals include apatite and magnetite.

The hornblende diorite shows alteration products similar to those in the metamorphic rocks. Hornblende has altered to chlorite and some epidote with the formation of magnetite from released iron. The poikilitic texture (Figure 16) of hornblende with blebs of albite and quartz commonly seen in the amphibolites is also present in the diorite. Saussuritization of plagioclase with development of sericite and epidote is also common. The similarity of alteration minerals and their textures to the metamorphic rocks suggest the cause and conditions were similar. This and the granitic dikes observed cutting the diorite show that the diorite is older than the biotite granite.

Two hornblende diorite dikes petrographically very similar to the hornblende diorite pluton are exposed in the northeast corner of the area on the Red Bluff Mine properties.

Hornblende Biotite Granodiorite

Hornblende biotite granodiorite is exposed on the west side of the Black Rock granitic intrusion approximately one kilometer west of Black

Rock. The grayish-white exposure of soil and bedrock is in a round drainage basin three quarters to one kilometer in diameter. The foundations of the old mining town of Constellation are in this drainage depression.

The hornblende biotite granodiorite has a medium grained hypidiomorphic granular texture composed of plagioclase, quartz, microcline, biotite, and hornblende (Figure 18). A compositional plot according to Streckeisen (1976) is shown in Figure 19. Plagioclase compositions are in the andesine range averaging An_{34}. Subhedral laths of andesine up to 3mm (.118 in.) in length are well twinned, often zoned, and constitute approximately 35% of the rock. Andesine grains can be as small as .2mm (.008 in.) in length. Surrounding the plagioclase laths are poorly twinned microcline grains and anhedral quartz grains. Microcline and quartz are roughly equal in proportion and together compose 40% of the rock. Biotite flakes range from small grains .25mm (.010 in.) in width to grains 1.6mm (.063 in.) in width. Biotite and hornblende each comprise 10-12% of the rock. Hornblende grains are as small as .2mm (.008 in.) and reach 10mm (.394 in.) as euhedral phenocrysts. It is possible some of these hornblendes are xenocrysts incorporated from the amphibolites. A similar situation occurred in a mafic border phase of the Black Rock granite (see below). However, these hornblendes are pleochroic in shades of brown whereas the amphibolite hornblendes are blue-green. Brown hornblendes are typical of the oxidizing igneous environment and blue-green hornblendes are typical of the reducing metamorphic environment. Apatite, magnetite, and sphene are common accessory minerals.

Alteration of the primary igneous minerals is light. Sericitization of andesine occurs, but rarely is the whole grain completely altered.

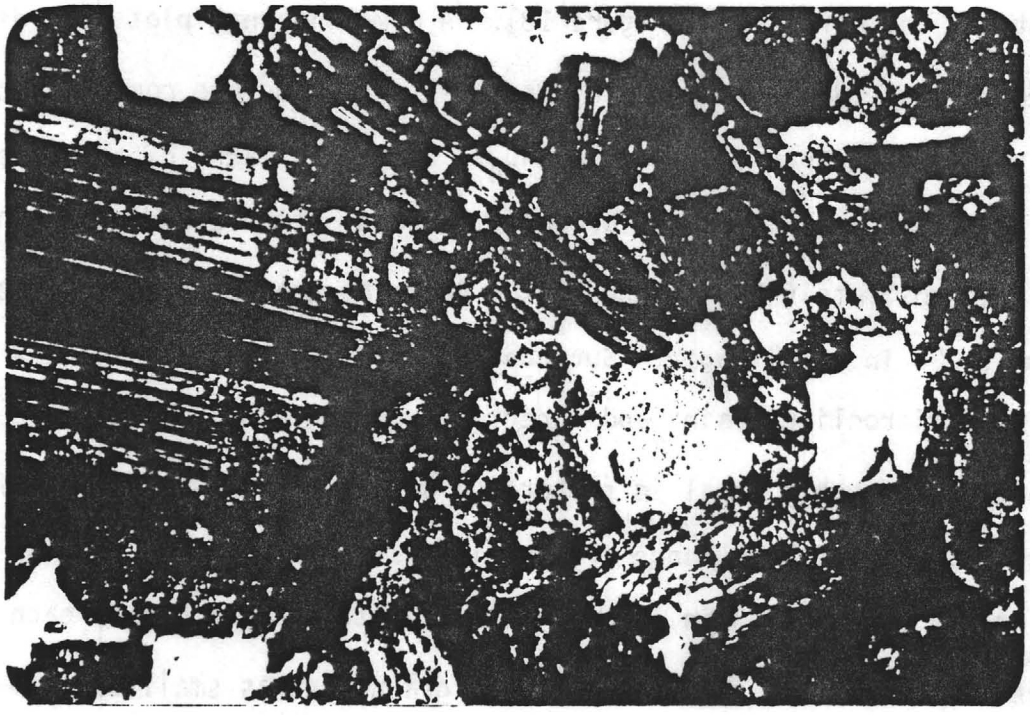

Figure 18. Photomicrograph of Hornblende Biotite Granodiorite Textures and Mineralogy. 50x.

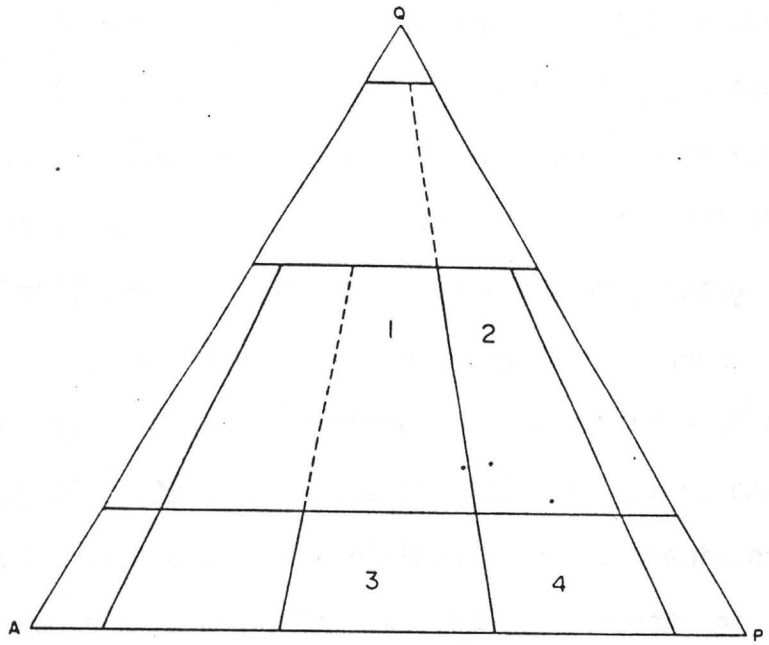

Figure 19. QAPM Compositional Plot (Streckeisen, 1976) of Three Hornblende Biotite Granodiorite Samples. 1 = Monzogranite, 2 = Granodiorite, 3 = Monzonite, 4 = Monzodiorite.

Similarly, chloritization of the biotites and hornblendes occurs but is not extensive. The degree and type of alteration can be attributed to deuteric alteration.

Black Rock and Long Ridge Granites

In the southwest and southcentral portions of the area are two granitic intrusions, the Black Rock and Long Ridge granites (informal names), respectively. They exhibit similar petrographic and field characteristics and intrude into amphibolite as well as granitic gneiss. The Black Rock granite developed a border phase of hornblende biotite quartz diorite, whereas the Long Ridge granite has not.

The Black Rock and Long Ridge granites exhibit a medium grained porphyritic xenomorphic granular texture (Figure 20). Plagioclase and perthitic microcline approach a hypidiomorphic character, but the rock is xenomorphic in general. Porphyritic microclines are commonly 2 to 3mm (.098 in.) in length, but can reach lengths up to 1cm (.394 in.), enhancing a primary flow foliation. Microcline constitutes 35 to 40% of the rock, plagioclase (oligoclase) 20 to 23%, quartz 25 to 27%, and biotite 8 to 10%. A compositional plot according to Streckeisen (1976) is shown in Figure 21. Quartz, plagioclase and biotite ranging from .2mm to 2mm (.008 and .080 in.) in width, interstitial to larger microcline and quartz is common in both granites. The larger microcline and quartz are between 2 and 3mm (.098 in.) in maximum length. Magnetite, sphene, and apatite are common accessory minerals.

On the eastern margin of the Black Rock granite, a more mafic phase (hornblende biotite quartz diorite) of the intrusive body has developed where it is in contact with a sizeable body of amphibolite. The contact

Figure 20. Photomicrograph of Black Rock and Long Ridge Granite Textures and Mineralogy. 50x.

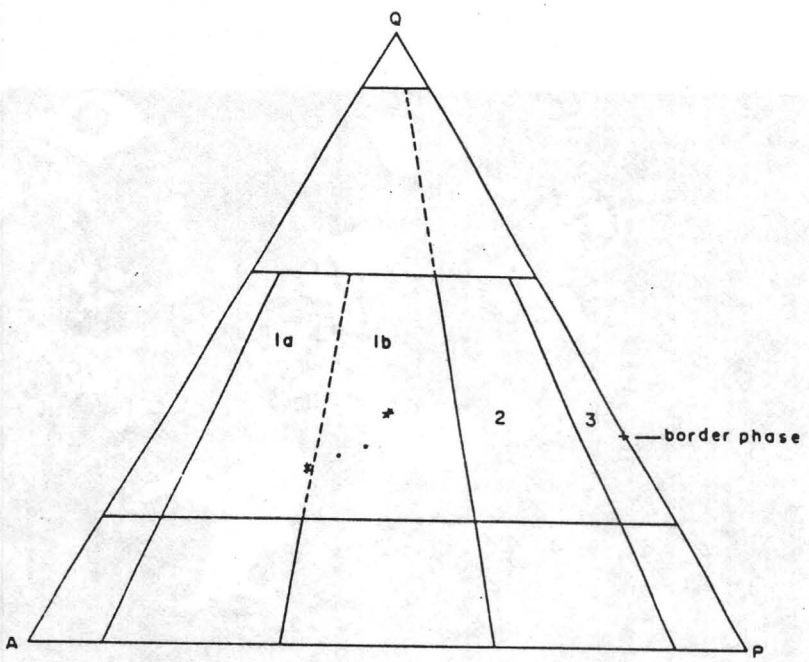

Figure 21. QAPM Compositional Plot (Streckeisen, 1976) of Five Samples of the Black Rock and Long Ridge Granites. * = Black Rock Granite, · = Long Ridge Granite, 1a = Syenogranite, 1b = Monzogranite, 2 = Granodiorite, 3 = Quartz Diorite.

is well exposed in King Solomon Gulch, south of Black Rock, directly adjacent to the Buckhorn road (Plate 1).

The hornblende biotite quartz diorite is characterized by a medium grained granular texture. The compositional plot on the Streckeisen (1976) diagram is in Figure 21. Note that potassium feldspar is missing. Plagioclase feldspars make up to 40% of the rock, are nearly euhedral, and exhibit compositional zoning (Figure 22). Small plagioclase grains are zoned throughout the crystal. Larger plagioclases have a nonzoned core, are often sericitized, and are surrounded by a zoned rim. Both normal and reverse zoning were observed. These textures indicate disequilibrium. Hornblendes similar to those in the hornblende biotite granodiorite are often subhedral to euhedral, and are probably xenocrysts incorporated from the intruded amphibolite. Hornblende constitutes about 8 to 12% of the rock, and biotite 12 to 15%.

The contact between the pluton and the amphibolite clearly is intrusive. Brecciation of the amphibolites and incorporation of the xenoliths and xenocrysts has caused the granites to increase in mafic content to a hornblende biotite quartz diorite. Figure 23 shows the results of the brecciation clearly. Within 40 meters (130 ft.), the amphibolite becomes increasingly injected with granitic material, becomes brecciated, and then grades into the diorite with numerous xenoliths. This border phase then grades into normal granite with fewer and fewer xenoliths. That the dioritic border phase is due to partial assimilation of solid mafic material is evidenced by more mafic rock surrounding amphibolite, xenoliths (Figure 24). The assimilation is probably mechanical in nature. Physical breakdown of the amphibolite into xenoliths and xenocrysts would explain the hornblende present only in this phase of the

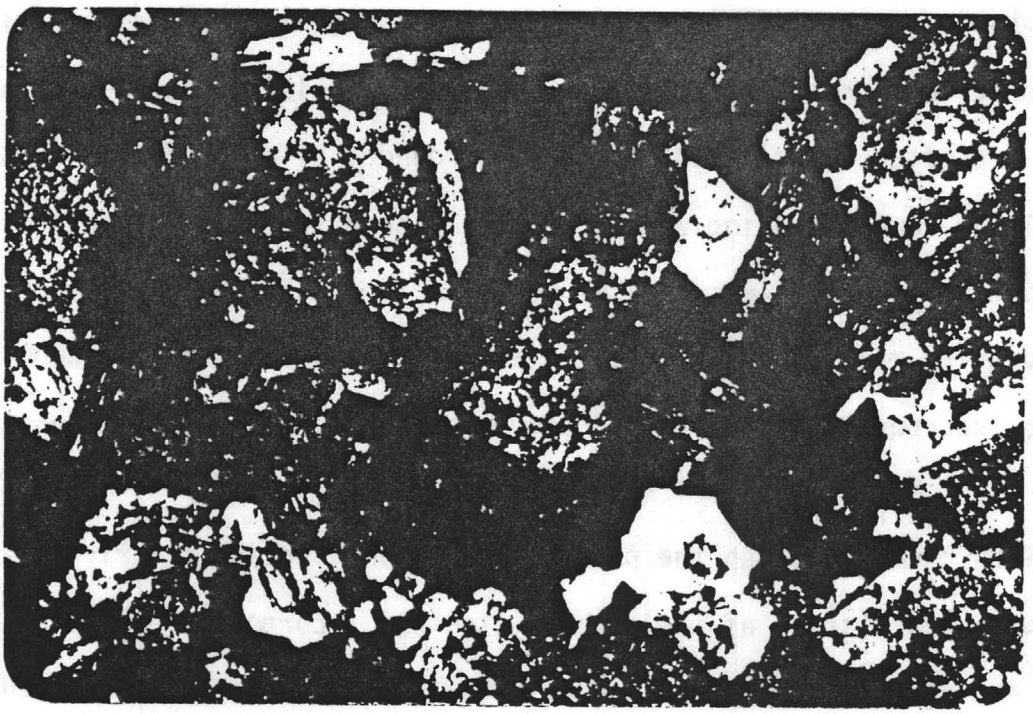

Figure 22. Photomicrograph of Black Rock Granite Border Phase Showing Zoned Plagioclase. 50x.

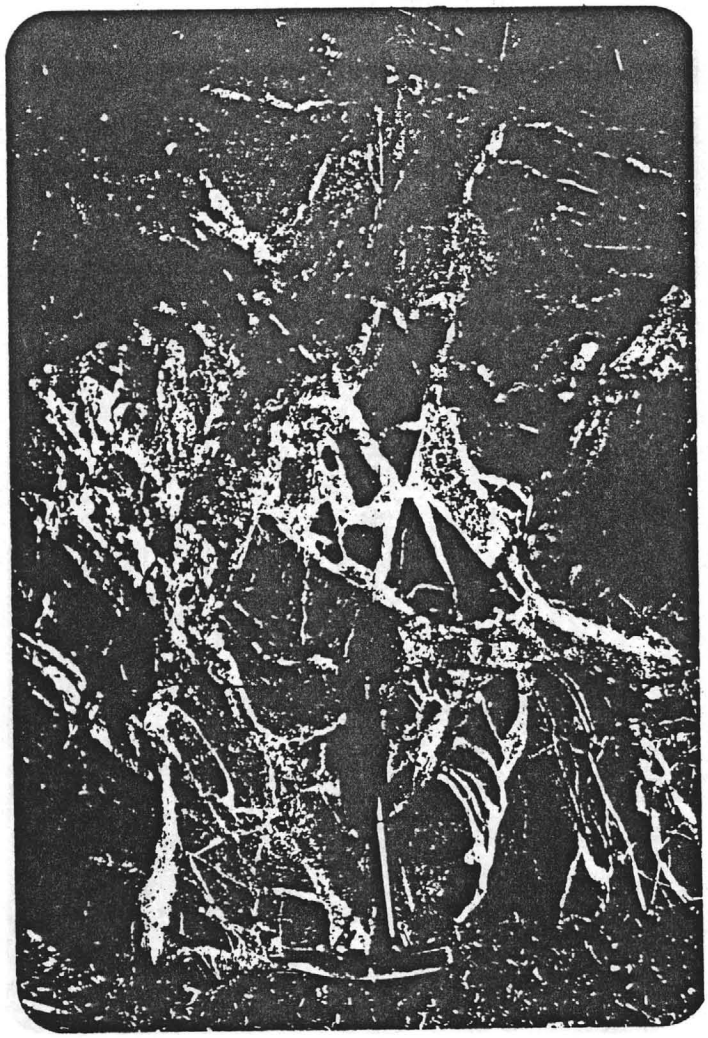

Figure 23. Photograph Showing Intrusive Brecciation of Amphibolite.

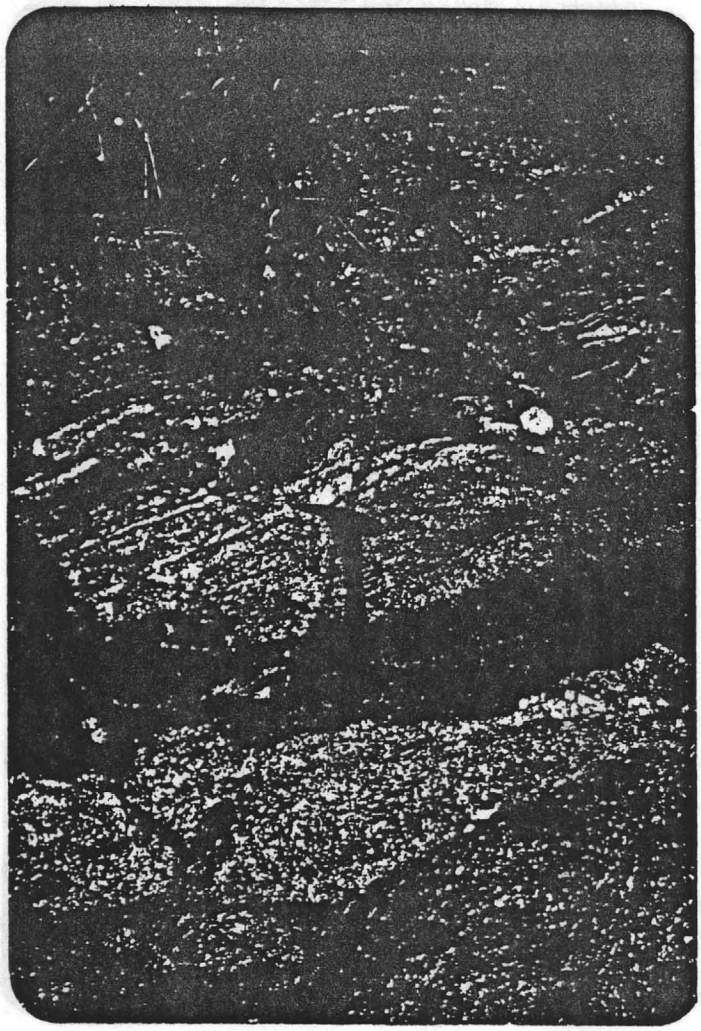

Figure 24. Photograph Showing Partial Assimilation of Amphibolite Xenoliths.

Black Rock intrusion. Depletion of felsic elements from granitic melts into incorporated mafic xenoliths has been documented (McBirney, 1979) and could explain the absence of K-spar in the Black Rock border phase.

The Black Rock and Long Ridge granites are only lightly altered, except when in close proximity to the Tertiary hydrothermal veins. The dominant alteration product of the plagioclase feldspars is sericite. Accessory amounts of epidote are present, indicating some saussuritization was occurring. Chlorite is common but not extensive as an alteration product of biotite and hornblende, when the latter is present.

Biotite Granite

Bordering the Morgan Butte area in the northern portions is a batholith of biotite granite. This batholith is extensive to the north of the area, as shown in Figure 1. The injected nature of the adjacent metamorphic rocks and the abundance of xenoliths in the granite define an intrusive contact. Along the contact, intrusion produced xenoliths up to 18 meters (60 ft.) in large dimension that have not fully separated or are still "floating" in proximity to the original mass of country rock. This area is mapped as a border zone due to its complexity. Many alaskitic late stage phases as well as normal granite and tourmaline pegmatites intrude this zone. The xenoliths are mostly of the granitic gneiss, although amphibolite xenoliths increase in abundance in the western part of the zone. Two similarly mapped zones are on the southeastern and southern edges of the area. Granite is known to be widely exposed to the south and east of the study area.

The representative phase of the biotite granite has a medium grained xenomorphic granular texture (Figure 25). Coarse grained

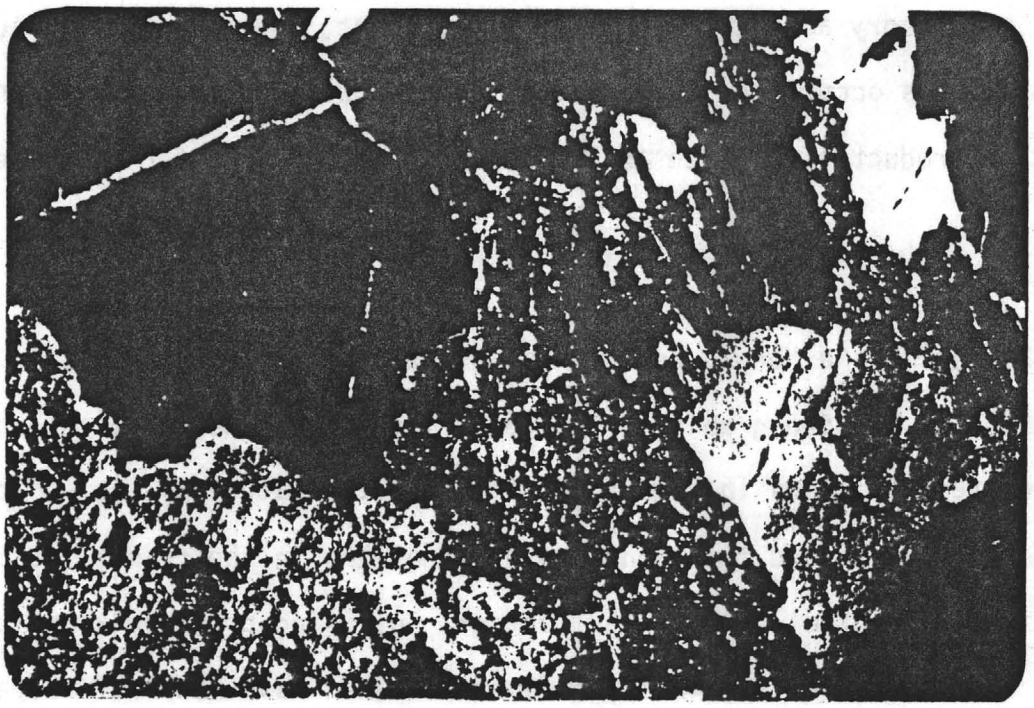

Figure 25. Photomicrograph of Biotite Granite Textures and Mineralogy. 50x.

varieties exist but are not as extensive. Finer grained alaskitic varieties are common along the contact in both the granite and the metamorphic rocks. In the representative phase, microcline phenocrysts can reach 12mm (.472 in.) in length, are usually 4 to 6mm (.157 to .236 in.) in length, and constitute 24 to 27% of the rock. Plagioclase feldspar (oligoclase) constitutes 24 to 31% of the rock, is typically poorly twinned, anhedral, and 2 to 6mm (.080 to .236 in.) in length. Quartz grains are anhedral, up to 3mm (.118 in.) in width, and commonly clustered in aggregates up to 12mm (.427 in.) in maximum dimension. Quartz makes up 35 to 38% of the rock. Biotite ranges from small shreds .3mm to 2.5mm (.012 to .098 in.) in length. Biotite flakes are typically in clots up to 4.5mm (.177 in.) in maximum length and comprise 9 to 10% of the rock. Note that the composition (Figure 26) trends towards a monzogranite. Accessory minerals include apatite, muscovite, zircon, and rare magnetite. Chloritization of biotite and sericitization of plagioclase occurs, but is not extensive.

The late stage varieties other than the pegmatites associated with the batholith exhibit variations on a medium grained xenomorphic granular texture. These derivative melts are common in the border zone, are present in the adjacent metamorphic rocks as evidenced by small granitic plutons and are common along the margin of the batholith. They occur as irregularly round bodies a few tens to a hundred meters in width, and as dikes up to 8 meters (26 ft.) wide. Biotite is present in accessory amounts or is absent, lending the late phases an alaskitic texture. Often medium grained tourmaline (schorl) is present and comprises as much as 6% of the rock.

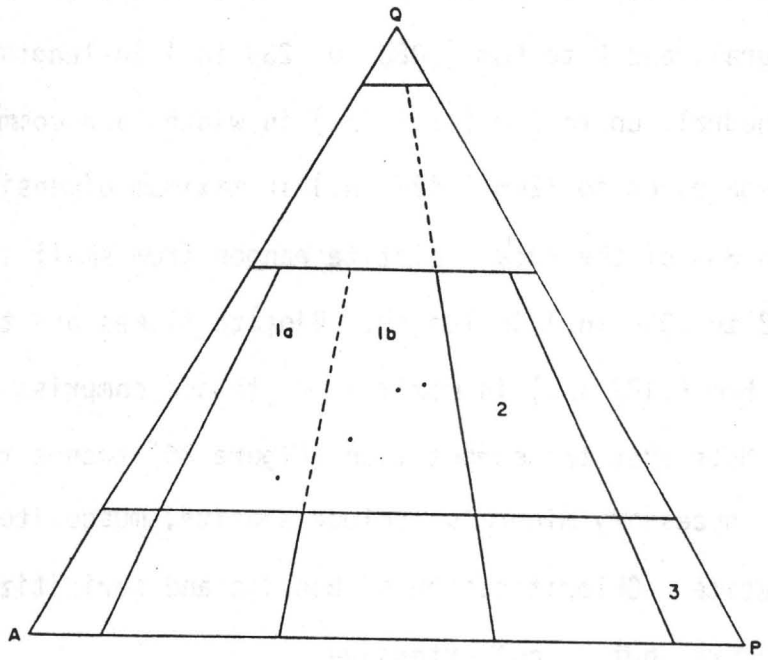

Figure 26. QAPM Composition Plot (Streckeisen, 1976) of Four Biotite Granite Samples. 1a = Syenogranite, 1b = Monzogranite, 2 = Granodiorite, 3 = Diorite, Gabbro.

Pegmatites intruding the older igneous-metamorphic terrane and the batholith itself are very common. Except for abundant tourmaline, the pegmatites are simple in composition and exhibit typical pegmatitic textures. Microcline and perthite crystals can reach a maximum length of 15cm (6.2 in.), quartz, approximately 6cm (2.4 in.), and muscovite occurs in tabular books up to 10cm (4 in.) in width. The long, narrow, black, tourmaline crystals can also reach 10 to 12cm (4.3 in.) in length and locally can be very abundant. Quartz and feldspar commonly occur in aggregates up to 25cm (10 in.) in long dimension. Zoning of the pegmatites is not common. The pegmatites occur as lenses and pods up to a few meters in width. In the metamorphic rocks the pegmatites are both concordant and discordant to the foliation and often have apophyses following the foliation.

Fine grained varieties that would classify as aplites are rare. Aplitic texture, where grains are numerous but small, is thought to be due to the absence of volatile content, particularly water (Hyndman, 1972). Since there is a paucity of aplites in the area it follows that volatiles are a significant factor in the intrusion of the batholith. The abundance of tourmaline pegmatites, medium grained intrusive bodies and the retrograde metamorphism of the intruded lithologies is attributed to this volatile content.

General Aspects of Pluton Chronology

The age of the plutonic rocks is considered to be Precambrian. This conclusion is based on crosscutting relationships and lithologic similarities. The biotite granite is probably correlative with the Crazy Basin quartz monzonite (1624 m.y., Blacet, 1968), 35 kilometers (22 mi.)

to the northeast. Both intrusions have similar compositions, intrusive characteristics, and contain exceptional amounts of tourmaline bearing late stage fluids. Figure 26 shows the composition of the batholith to be a monzogranite according to Streckeisen's (1976) classification system. The difference between a monzogranite and a quartz monzonite lies in the classification scheme used by the respective authors.

The contact between the batholith and the metamorphic rocks in the Morgan Butte area is definitely intrusive in nature. Xenoliths of the granitic gneiss and amphibolites are abundant in the batholith. The granitic dikes, pegmatites, and small granitic plutons are abundant throughout the metamorphic terrane as well as in the batholith itself. The tourmaline bearing pegmatites are more abundant closer to the batholith. Assuming that all of these tourmaline bearing pegmatites and the granitic dikes are genetically related to the batholith, four out of the five other plutonic igneous rocks can be shown to be older than the batholith. The pegmatites clearly cut the hornblende diorite, Black Rock granite, and the hornblende biotite granodiorite. Xenoliths of the hornblende biotite granodiorite in the Black Rock granitic intrusion also support the interpretation that the granodiorite is older than the biotite granite. The hornblende biotite granodiorite is probably similar in origin as the hornblende biotite quartz diorite phase of the Black Rock granite. The Black Rock and Long Ridge granites are considered to be synonymous in origin, making the Long Ridge granite also older than the biotite granite.

The pegmatites, however, are more abundant intruding the metamorphic rocks than the various plutonic rocks. Apparently the igneous rocks were less conducive to intrusion than foliated, fractured, and

sheared metamorphic rocks at the time of pegmatitic and granitic dike intrusion.

In the northeast corner of the area, on the Red Bluff mine properties, two exposures of fine to medium grained hornblende diorite dikes can be seen cutting both the metamorphic rocks and the biotite granite. Both dikes and the hornblende diorite body farther south are petrographically very similar. However, the pluton of diorite is evidenced to be older and at least one of the dikes to be younger than the biotite granite.

Chapter 4

TERTIARY UNITS

Introduction

Tertiary rocks in the Morgan Butte area include rhyolite porphyry dikes, mafic dikes, and hydrothermal vein deposits. The dikes are characterized by phenocrysts of several different mineralogies in a fine grained to aphanitic groundmass. The hydrothermal deposits have been heavily altered by supergene alteration processes subsequent to their deposition as discreet veins. The veins are associated both with and without the Tertiary dikes.

The veins and dikes are invariably northwest oriented and vertical to near vertical. They are associated with a prominent northwest structural fabric that crosscuts the Precambrian trends.

Rhyolite Porphyry Dikes

One of the prominent features defining the northwest trend is the rhyolite porphyry dikes. These dikes commonly extend for a kilometer or more, have near vertical dips, and are usually flow foliated parallel to the long dimension (Figure 27). The dikes are rarely less than 4 meters (13 ft.) and greater than 8 meters (26 ft.) wide. They often bifurcate or make an abrupt turn at an angle usually less than 35^{o}. All but a few crosscut Precambrian metamorphic foliation. Some dikes extending only one hundred to two hundred meters have a northeast strike. The dike cutting across the saddle on Morgan Butte exemplifies this.

Figure 27. Photograph Showing Flow Foliated Rhyolite Porphyry Dike.

One of the northwest trending dikes on Morgan Butte is for the most part vertical, but rolls over to a shallow northerly dip in the vicinity of an unnamed mine; and then is vertical again as it continues across the northern spur of the butte. This is possibly in response to a major flexure in the metamorphic foliation in the area.

The rhyolite porphyry dikes are light colored and fairly massive in outcrop. In thin section the groundmass is very fine grained to aphanitic with extremely variable amounts of subhedral to euhedral quartz phenocrysts up to 1.5mm (.059 in.) in width (Figure 28). Potassium feldspar phenocrysts of similar size are less common.

Mafic Dikes

The mafic dikes have the same northwesterly, near vertical strike as the rhyolite porphyry dikes, but exceptions are more common. The dikes do not extend as far on strike, and are not as wide as the rhyolite porphyry dikes. They commonly show an anastomosing relationship where they bifurcate into apophyses and pinchout or join with the main swarm again in an interweaving fashion (Figure 29). The mafic dikes show multiple intrusions whereas the rhyolite porphyry dikes do not. Chilled margins and flow foliated phenocrysts are common. Presumably differences in viscosity result in the differences in intrusive nature of the two types of dikes.

The mafic dikes have a variety of textures. Phenocryst sizes in a fine grained groundmass vary widely, even in the same dike. Plagioclase phenocrysts, typically 1mm (.040 in.), but up to 5mm (.197 in.) in length, are the most common. They are usually euhedral, and commonly altered to epidote. Euhedral augite up to 2cm (.787 in.) is less common, with

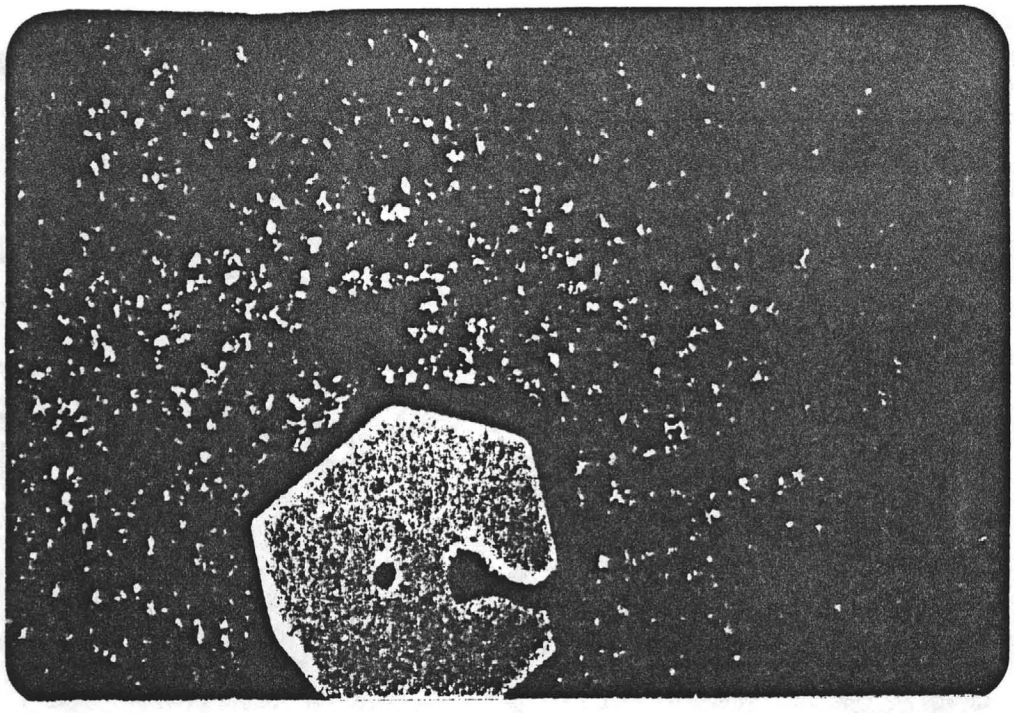

Figure 28. Photomicrograph of Rhyolite Porphyry Textures and Mineralogy. 50x.

Figure 29. Photograph Showing Anastomosing Mafic Dikes.

hornblendes and biotite even less abundant. Many dikes, especially the smaller ones, have no phenocrysts at all.

The mafic dikes are commonly associated with hydrothermal activity. Where this is the case, the dikes are usually altered to an aphanitic chloritic-hematitic groundmass with a hint of relict phenocrysts.

Hydrothermal Vein Deposits

Vein Mineralogy

Primary vein minerals in decreasing order of abundance are: quartz, pyrite, chalcopyrite, calcite, siderite, fluorite, galena, arsenopyrite, and tetrahedrite. Zinc is reported (Keith, 1969) to occur in the Morgan Butte area, but no sphalerite was observed in the samples collected. Bastin (1922) studied the Monte Cristo mine and reported the nickel arsenides, niccolite (NiAs), chloanthite ($(Ni,Co)As_{3-x}$), and gersdorfite (NiAsS), as well as tennantite ($(Cu,Fe,Zn,Ag)_{12}As_4S_{13}$), enargite ($Cu_3AsS_4$), proustite ($Ag_3AsS_3$), pearceite ($Ag_{16}As_2S_{11}$), barite, argentite ($Ag_2S$), and primary native silver. Microscopic gold is present in the veins in highly variable amounts.

The vein deposits apparently have been heavily altered by supergene processes. Secondary specularite, intergrown with chrysocolla is a common alteration product of the veins in the northeast parts of the area. Throughout the rest of the area, secondary quartz, calcite, limonite, specularite, and amorphous hematite, are the typical products of alteration. The copper carbonates, malachite and azurite are common and turquoise was mined from the Chinaman claim, near the Red Bluff mine properties. Erythite (cobalt bloom) and annabergite (nickel bloom) are reported from the Monte Cristo mine (Bastin, 1922). Limonite pseudomorphs

after pyrite, comb structure quartz, and bladed malachite are typical secondary textures. Gold tends to be residually enriched above the water table with the removal of oxidized soluble elements. Secondary uranium minerals are reported from the Abe Lincoln mine (Pierce, 1970), as well as native copper. The veins after the supergene alteration, range in width from a few millimeters (tenths of inches) to roughly a meter (3 ft.) in thickness. They pinch and swell drastically and vein shoots tend to thin rapidly.

Alteration

Sericitic alteration, as much as four meters (13 ft.) to either side of some veins, has produced abundant sericite and pyrite in the Precambrian wall rock. Chlorite and epidote, typical of propylitic alteration are equally widespread. The proportions of each alteration product varies with the wall rock compositions, regardless of age. More detailed work on the vein deposits may show that the alteration is zoned. Groundwater oxidation of the veins and their alteration haloes has produced abundant limonite and amorphous hematite that is a conspicuous rust red gossan in contrast to the white and gray Precambrian rocks (Figure 30).

Descriptions of Vein Deposits

Introduction. The vein deposits have been grouped together to correspond with three northwest structural trends and similarities in supergene alteration:

1. The Denver Hill Group is in the southernmost portion of the area and includes the Keystone Mine. The Keystone Mine is on an adjacent, but similar, trend.

Figure 30. Photograph Showing Rusted Gossan of a Hydrothermal Vein.

2. The Slim Jim Group passes through the center of the area and includes the Monte Cristo Mine, the Black Rock Mine, the long fault zone on the south side of Slim Jim Creek, and an unnamed mine in upper Slim Jim Creek. The Abe Lincoln is also on this trend, but is just outside the southeast boundary of the mapped area.
3. The Red Bluff trend passes through the northern portions and probably includes the Gold Bar Mine, however, that mine was not open to inspection.

Denver Hill Group. The Denver Hill Group is associated with a swarm of rhyolite porphyry dikes and a smaller amount of mafic dikes. Denver Hill itself is a northwest trending topographic expression of these dikes. A faulting structural control of emplacement of the dikes and migration of hydrothermal fluids is evident from brecciation and slickensides. Although supergene alteration of the vein deposits has obscured many of the fault textures, slickensides suggest a vertical to near vertical displacement. Brecciated and altered country rock includes both Precambrian and Tertiary rocks, the latter being more abundant.

Supergene alteration by oxidizing groundwaters has favored the assemblage of quartz, limonite, amorphous hematite, malachite and azurite. The copper carbonates often form excellent bladed, fibrous, and plate-like crystals.

Slim Jim Group. Relations between faulting, dikes and veins are complex. The association of vein minerals with the dikes is strong, but not as consistent as in the Denver Hill Group. In lower Slim Jim Creek

veins are present with and without the Tertiary dikes. Rhyolite porphyry dikes dominate. In upper Slim Jim Creek, veins are with and without the dikes, and mafic dikes are more abundant. It is very likely that the Slim Jim Group of veins is on a trend where there are several parallel and/or interbranching zones of faulting, dike emplacement and vein deposition. Supergene alteration on these veins is strong and gossan at the surface is particularly striking. Limonite and amorphous hematite are very common. The specularite and chrysocolla association is present but not as common as in the Red Bluff area. Malachite and azurite are not as well developed and not as common as in the Denver Hill Group.

Red Bluff Group. The association between the veins and Tertiary dikes is not as evident on the Red Bluff trend. Rhyolite porphyry and mafic dikes are in the area but are generally not in direct proximity to the major veins. Vertical to near vertical faulting, as evidenced by brecciation and slickensides occurs with both. Secondary limonite, amorphous hematite, and intergrown chrysocolla and specularite, exhibit some slickensided surfaces, suggesting repeated fault movement as recent as the supergene alteration of the vein. Rebrecciated breccia fragments that had been altered and cemented by hypogene hydrothermal processes, also indicate repeated faulting.

The Red Bluff claims, 2.4 kilometers (1.5 mi.) north of Morgan Butte, are on some major veins associated with northwest faulting. The vein/fault zone corresponds with a change of lithology. Biotite granite, with numerous stoped xenoliths of the gneiss and often with flow foliation, is in apparent fault contact with foliated quartzo-feldspathic gneiss with numerous amphibolite metaxenoliths that is injected extensively with pegmatitic and granitic dikes. Evaluating displacement between such

subtly different and horizonless fault blocks is difficult. However, the major vein/fault zone in Amazon Gulch also truncates a medium grained hornblende diorite dike that is believed to be Precambrian in age (see General Aspects of Pluton Chronology).

There is a compositional difference between the veins on either side of the fault. The veins on the southwest side of the fault tend to contain more copper, yielding abundant chrysocolla and some turquoise (Chinaman Mine) upon supergene alteration. On the northeast side, gold content is higher and copper low. The veins tend to have quartz-specularite-limonite-calcite assemblages upon alteration. Whether this trend is a function of the differing host rocks or juxtaposition of differing veins due to faulting is unknown.

Northwest of the Red Bluff Mine, the veins exhibit more hypogene vein minerals and textures than any others in the area. Normally, to find samples of vein material in the hypogene state, one must pick through the mine dumps. However, a number of veins with test pits a few meters (10 ft.) deep, yielded samples with unaltered chalcopyrite, pyrite and tetrahedrite. The reason for this anomaly is unknown.

Vein Origin

The vein deposits are closely associated with the late Tertiary structures superimposed on the Precambrian grain. The strong northwest trend, as defined by the rhyolite porphyry dikes, mafic dikes, vertical to near vertical faulting, and oxidizing vein zones is related to the tectonovolcanic depression of the adjacent Castle Hot Springs volcanics (Figure 31). These volcanics are exposed in a northwest trending graben that passes by the Morgan Butte area on the northeast boundary. A Mio-

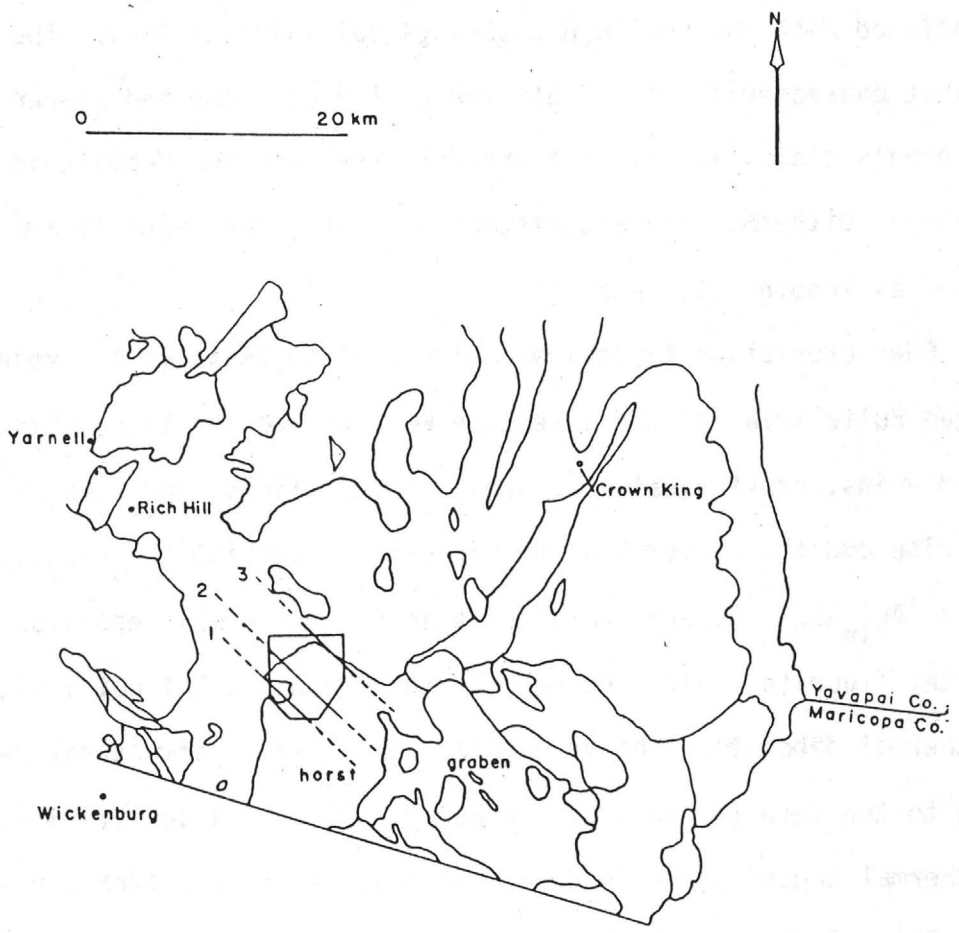

Figure 31. Map of South Central Yavapai County Showing the Horst and Graben Relationship Between the Morgan Butte and Castle Hot Springs Areas. Adopted From Map 3-10, Geologic Map of Yavapai County, Arizona, Bureau of Geology and Mineral Technology, Tucson. CHSv = Castle Hot Springs volcanics, Trend 1 = Denver Hill Group, Trend 2 = Slim Jim Group, Trend 3 = Red Bluff Group.

cene (?) age for the volcanics is proposed by Ward (1977).

The vein deposits have been deposited from hydrothermal emanations associated with the Castle Hot Springs volcanic activity. The deposits exhibit characteristics of both the epithermal zone and deeper zones of Lindgren's classification, as presented by Park and MacDiarmid (1975). Although epithermal characteristics dominate, the deposits are best classified as xenothermal in origin.

Characteristics typical of epithermal deposits in the veins of the Morgan Butte area include extensive wall rock alteration, sharply defined veins, crustifications, open space fillings, and comb structures. Siderite and the silver bearing minerals, proustite (Ag_3AsS_3), and pearceite ($Ag_{16}As_2S_{11}$), are characteristic of epithermal deposits. Chalcopyrite, fluorite, gold, and galena are common in, but not limited to, epithermal deposits. The veins also have a close structural relationship to the late Tertiary Castle Hot Springs volcanic activity. Many epithermal deposits are in or around centers of late Tertiary volcanism.

Several characteristics are more indicative of a deeper zone of emplacement. Bastin (1922) reported that extensive replacement of the Precambrian granitic gneiss has occurred in the Monte Cristo mine. Replacement is more common than open space fillings in mesothermal deposits. The abundance of the base metal sulfides and the presence of tennantite and enargite, although not unknown in epithermal deposits, is also more typical of mesothermal deposits.

A depth of origin deeper than the epithermal zone, however, would require the removal of at least 1,000 meters (3,000 ft.) of overburden since deposition of the hydrothermal minerals. Ward (1977) has shown that the late Miocene (?) faulting that formed the Castle Hot Springs

graben (and controlled emplacement of the veins in the Morgan Butte area) was active in the last stages of the volcanic activity in that area. The horst of Precambrian rocks in which the veins occur was structurally adjacent or nearly adjacent to the volcanics at the time of vein deposition. Figure 31 shows the relationship between the horst and graben. The volcanics reached a thickness of at least 400 meters (Ward, 1977) in the Miocene; of this thickness little appears to have been removed by erosion. This suggests that the vein deposits formed during the latest stages of volcanism were formed at epithermal depths.

A xenothermal origin is evidenced by telescoped mineral assemblages that formed at a depth in the epithermal zone. Minerals more characteristic of deeper, hydrothermal veins have been reported in and around the Morgan Butte area. Nickel arsenides are reported from the Monte Cristo mine (Bastin, 1922) and Lindgren (1926) reported bismuthinite on hearsay evidence from the Swallow mine a few kilometers to the northeast of the area. A "tungsten trend" from Castle Hot Springs to Yarnell, Arizona has been a target of exploration groups and prospectors for years.

Specularite has been reported as a primary vein mineral (Bastin, 1922), but is also clearly a secondary alteration mineral intergrown with chrysocolla in the northeast parts of the Morgan Butte area. Bastin (1922) reported primary native silver, proustite (Ag_3AsS_3), and pearceite ($Ag_{16}As_2S_{11}$), occurring with the nickel arsenides, niccolite (NiAs) and Chloanthite ($(Ni,Co)As_{3-x}$), without replacing them. Bastin (1922) noted that several ore types are recognizable, and that there is no clear evidence of more than one general period of primary mineralization.

On the basis of the telescoped mineralogies and textures, the deposits are classified as xenothermal in origin, in the belief that more detailed work on their mineralogies, paragenesis, and spatial relations will corroborate this interpretation.

Summary

Relations between the vein deposits, rhyolite porphyry dikes, mafic dikes and faulting are complex. They invariably are northwest oriented. Crosscutting relationships show rhyolite porphyry intruded by mafic dikes, altered and mineralized by hydrothermal solutions, and brecciated by faulting. Some rhyolite porphyry dikes are fresh and continuous for over 1,000 meters (3200 ft.), but were not conclusively observed to cut mafic dikes or vein zones. The mafic dikes are both altered by and crosscut the vein deposits, although the latter is rare. Brecciated fragments in a vein near the Gold Bar Mine in the northwest part of the area, show alteration rims and primary mineral deposits in the remaining spaces. The deposits and breccia fragments are fractured again, parallel to the vein, suggesting faulting and vein deposition to be contemporaneous, at least in part. Elsewhere, secondary chrysocolla and limonite exhibit near vertical slickensides, suggesting more recent repeated movement along the same fracture zones. In general, however, supergene processes and subsequent development of secondary minerals have obscured fault textures.

Chapter 5

STRUCTURAL ELEMENTS

Introduction

Structural elements associated with the Precambrian metamorphic events include a pervasive foliation (S_1) throughout the metamorphic rocks and sparse small scale folds or kinks, with one major flexure (F_1). The F_1 structures are defined by the S_1 foliation. A mineral lineation (l_1), defined by prismatic hornblende, is rare. The lineation is recognizable in the field only in the coarser grained phase of the amphibolites, which is subordinate to the finer grained phase. Aside from the basite xenoliths in the premetamorphic granite an S_0 surface, such as bedding, is unrecognizable. Both the amphibolites and granitic gneiss are essentially massive.

The Precambrian plutonic rocks are commonly flow foliated (P_1) along the margins of the intrusions. No recognizable Precambrian faults were observed, although northeast to easterly trending shear zones are common. The shears are commonly obscured by Tertiary hydrothermal activity. Joint orientations are complex, but show near vertical sets trending northeast and northwest.

Tertiary structural elements are strongly northwest oriented (Plate 1). The trend is defined by faulting and fracturing controlling parallel dike and hydrothermal vein emplacement.

Foliation (S_1) and Lineation (l_1)

Metamorphic foliation (S_1) is pervasive throughout the amphibolites and granitic gneiss. The S_1 surface is defined by hornblende, plagioclase, and less commonly, biotite, in the amphibolites. A weak compositional banding of hornblende and plagioclase, parallel to the mineral orientation, adds to the fabric. The hornblende crystals are typically oriented randomly within the S_1 surface, but in the rare, coarser varieties, they can define a mineral lineation (l_1, Figure 32). The coarser varieties are typically more granoblastic, however. When biotite is present, its lepidoblastic fabric also contributes to the S_1 surface. Foliation in the granitic gneiss is defined primarily by oriented biotite and a compositional banding between biotite and quartzofeldspathic material. When potassium feldspar is blastoporphyritic, the texture is augenlike.

The foliation measurements are plotted on an equal area net in Figure 33. Although the overall distribution shows the foliation striking east and dipping steeply north, the northwest portion of the metamorphic terrane is characterized by a northeast foliation. The southern and eastern portions show eastsoutheast foliations. The small high in the center of the diagram is caused by the near horizontal limb of a major flexure on Morgan Butte.

The transition from the northwest to the northeast corners of the metamorphic terrane shows the foliation strike changing from northeast to eastsoutheast. The strike of the boundary into the biotite granite batholith also shows this change, suggesting a relation between the two. On the scale of the whole mapped area, the foliation demonstrates this

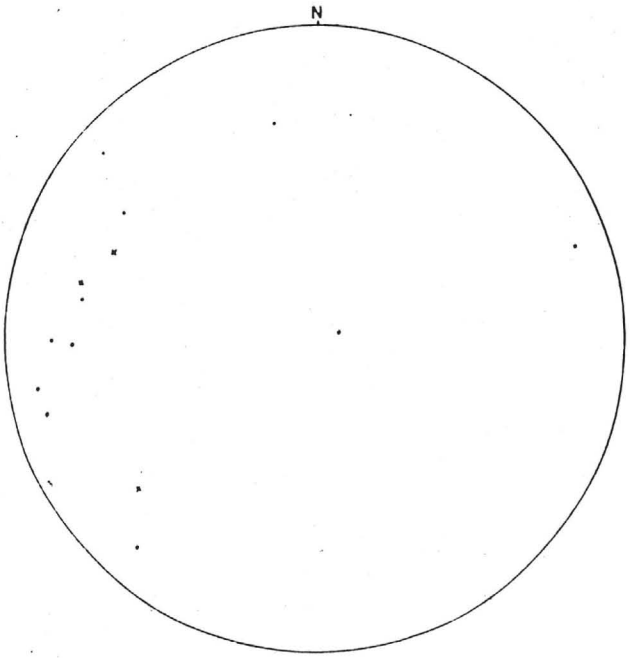

Figure 32. Plot of Linear Features on an Equal Area Net. x = Mineral Lineations (l_1), · = Small Fold and Kink Axes, and the Major Flexure Axis (F_1).

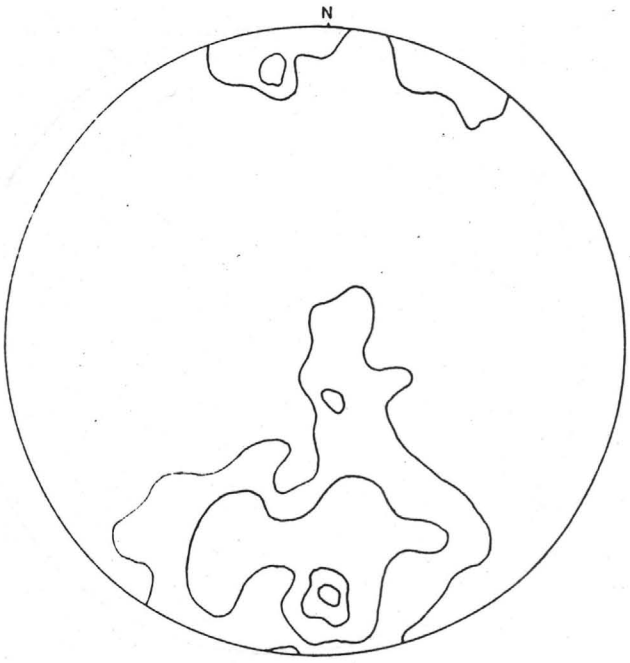

Figure 33. Plot of Pole to 134 Metamorphic Foliations (S_1) on an Equal Area Net. 2, 6, 10, 12 Count Contours.

northeast to eastsoutheast change in strike (Plate 1). However, on a local scale, the foliations are consistent across any lithologic changes. The pervasive S_1 foliation and F_1 features have developed without regard to lithologies.

Instances where a mineral lineation is defined by hornblende prisms are not common and in addition an exposure of the foliation surface is necessary for accurate measurement. This kind of exposure typically occurs in the creek bed exposures due to the vertical to near vertical nature of the foliations which contain the lineations. The few accurate measurements that were obtained are plotted with F_1 measurements in Figure 32. The lineations, like the F_1 features, plunge shallowly to the west.

Although minor in areal extent, an S_2 fluxion foliation can be assigned to cataclastic rocks in the northwest trending Tertiary faults. Cataclastic rocks exhibit textures ranging from mylonites to unconsolidated breccias (Higgins, 1971). Fault textures are commonly obscured by Tertiary hydrothermal activity.

Drag Folds, Kinks, and a Flexure (F_1)

Superimposed on the S_1 foliation surface are small scale drag and kink folds (Figure 34), and one major flexure. The deformation is defined by folded S_1 foliation surfaces. Although the small scale folds and kinks are not commonplace, they become more abundant on the limbs and hinge of the major flexure. Figure 32 is an equal area net plot of the attitude of the F_1 structures. The trend is to plunge gently northwesterly to southwesterly.

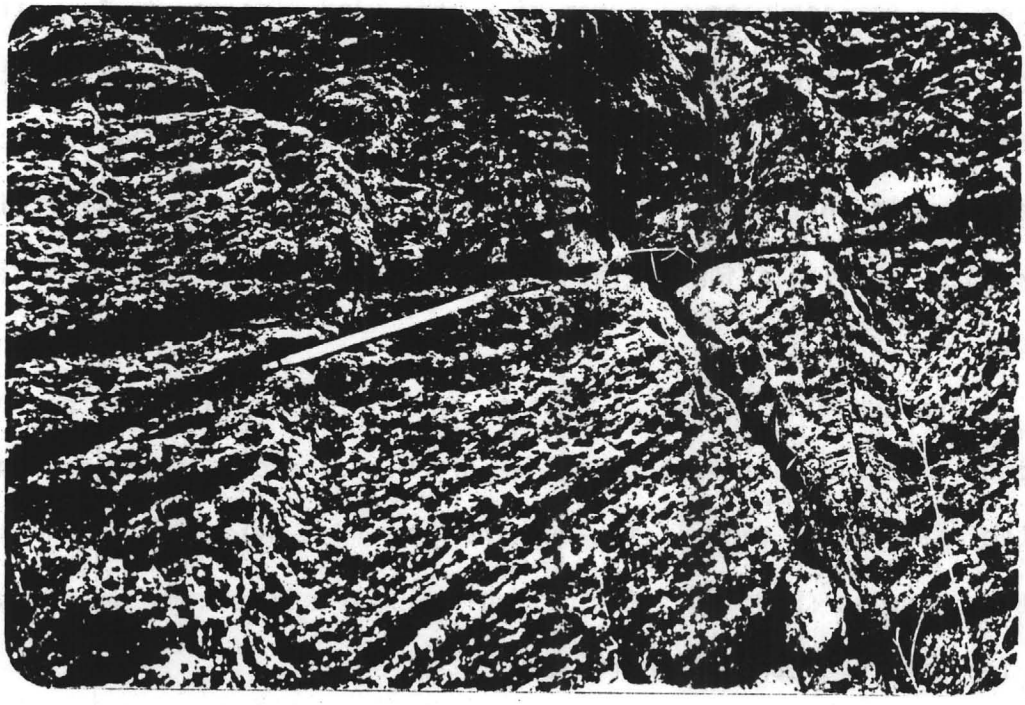

Figure 34. Photograph Showing Small Scale Fold in Granitic Gneiss.

The major flexure is exposed on the crest of Morgan Butte. Appendix II shows a geometric construction of the flexure axis from a representative average of foliation readings on each limb. It strikes N56^{o}W and plunges 13^{o}. The lower limb is typical of the foliation attitudes of the area in general. The limb trends eastsoutheast and dips steeply to the northnortheast. The lower limb makes up the foundation of Morgan Butte upon which the remnant of the upper limb lies (cross section, Plate 1). The upper limb caps the upper 150 meters (500 ft.) of northwest Morgan Butte, trends north-northeast, and dips very shallowly to the northwest. The hinge zone is exposed in the gullies draining west off of Morgan Butte. The exposures show it to be on the order of 3 meters (10 ft.) wide and extremely contorted. Figure 35 shows its contorted nature, which gives widely diverse and conflicting readings.

Joints

Fracture orientations are not without patterns, but are quite diverse. Some outcrops, particularly in the granites show a definite pattern of joints, but many show a complex pattern that lends the outcrop a chopped appearance. In some cases old joint patterns are rehealed with fresher patterns superimposed on the rock (Figure 36). Figure 37 shows equal area net plots of joint measurements taken in the area. There is a marked concentration of vertical to near vertical joints trending northeast and a set trending northwest and dipping steeply southwest. Numerous other orientations are scattered around the equal area net, showing the rather heterogeneous orientations of joints.

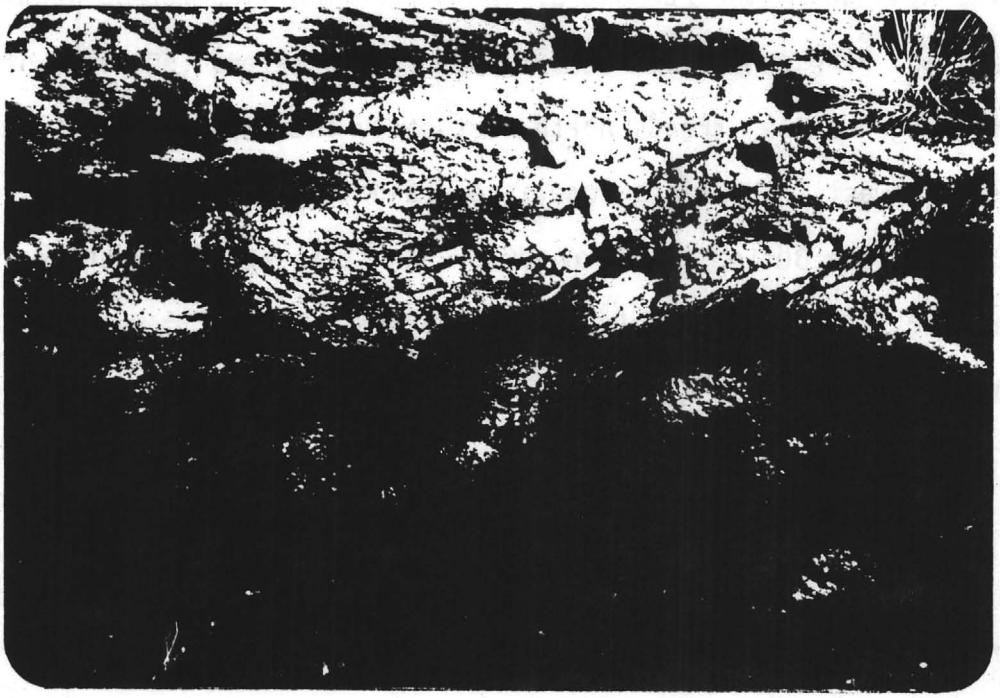

Figure 35. Photograph Showing Contorted Granitic Gneiss in the Hinge of the Major Flexure.

Figure 36. Photograph Showing Rehealed Joints.

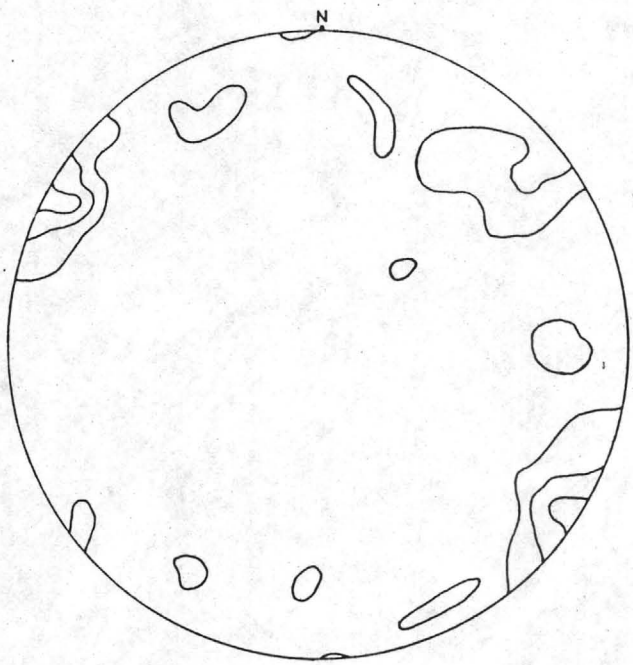

Figure 37. Plot of Pole to 62 Joint Planes on an Equal Area Net. 2, 6, 12 Count Contours.

Origin of Joints

For the most part, it is unknown which particular joint pattern was a result of which tectonic episode in Arizona history. Stresses during the late Cretaceous and early Tertiary epochs involved regional northeast-southwest compression followed by extension in the same direction during the late Tertiary epochs (Wilson, 1962). These extensional stresses led to the development of the Basin and Range Province. The northwest trending fabric that controlled the formation of the Castle Hot Springs graben; and in the Morgan Butte area, the normal faulting, dike emplacement and vein emplacement is related to the Basin and Range tectonic regime. The northwest trending set of joints that dip steeply southwest are probably related to this tectonic episode. The northeast trending joints could possibly be related to northwest extension associated with northeast compression. Older tectonic episodes cannot be correlated with any joint patterns.

Faults

Faults that can definitely be assigned a Precambrian age were not recognized in the area. Visible displacement along any possible faults is near impossible to discern, due to the horizonless fabric of the rocks.

However, minor shear zones of widely varying attitudes are common throughout the area. The shears can be recognized by closely spaced, interweaving fractures, chopping the rocks into complex zones. Commonly, these zones have been affected by mild hydrothermal activity. Undoubtedly, some of these shear zones are associated with the Precambrian events represented in the area, but they cannot be distinguished from shears developed during later tectonic episodes. However, shearing obviously

associated with the northwest-trending Tertiary dikes and faulting, can be assigned a Tertiary age.

Several northwest trending faults have been recognized and have been assigned a Tertiary age. These faults are vertical to near vertical and have had a profound structural control on dike and vein emplacement. The northwest trend is associated with the development of the Castle Hot Springs graben and has been assigned a Miocene (?) age by Ward (1977).

In the Morgan Butte area, at least 3 major faults or fault zones have been recognized (Figure 31). These three zones; the Denver Hill, Slim Jim, and Red Bluff trends, correlate with major zones of vein emplacement and are discussed in more detail in the section entitled Description of Deposits. Aerial photos of the Morgan Butte and outlying areas show these trends are not limited to the thesis area.

If these fault trends are actually complex zones of structural weakness, as is evidenced in Slim Jim Creek, then several trends become apparent (Figure 31). The Slim Jim trend encompasses the Monte Cristo mine within the area and the Abe Lincoln mine one half kilometer (.3 mi.) outside the southeast boundary of the area. The trend then follows Buckhorn Creek for 5 kilometers (3 mi.) to the southeast before entering the Castle Hot Springs volcanic area. The Red Bluff trend is a bifurcation of the larger Swallow Mountain trend, upon which several isolated volcanic buttes, as well as the Swallow and Whipsaw mines lie. Two kilometers (1.2 mi.) to the northeast of the Red Bluff trend lies the Castle Creek trend, along which Castle Creek flows southeast into the Castle Hot Springs area for at least 14 kilometers (8.6 mi.). Along all these trends are numerous springs.

The well known deposits of Rich Hill at Stanton and Octave, Arizona also lie on the same trend 20 kilometers (12.5 mi.) to the northwest, across the Hassayampa River.

Primary Flow Foliation (P_1)

Primary igneous flow foliation is common along the periphery of several of the plutonic intrusions in the area. Flow foliation is almost pervasive in the Long Ridge granite. The primary flow is usually roughly parallel to the plutonic border. The foliation is defined by roughly aligned microcline phenocrysts and a subtle foliation imparted to the normally granular matrix. At the pluton boundaries the width of flow foliated zones varies from tens of meters to hundreds of meters before grading into a normal granular igneous texture. Often the injected granitic material in the metamorphic rocks is flow foliated to the dike morphology and is often slightly oblique to the metamorphic foliation.

Figure 38 is an equal area net plot of flow foliations taken from the Black Rock, Long Ridge and biotite granites. The orientations in general are east-west and dipping at an intermediate angle to the north.

Summary

The S_1 foliation and l_1 mineral lineations are structural elements formed during metamorphism of the basites and the premetamorphic granitic intrusion. Defined by the S_1 foliation are small scale folds and kinks, and a major flexure (F_1). The F_1 structures are possibly related to the forceful intrusion of the biotite granite batholith. Primary flow foliation (P_1) developed along the periphery of many of the silicic intrusions, when they were a partially solidified crystal mush.

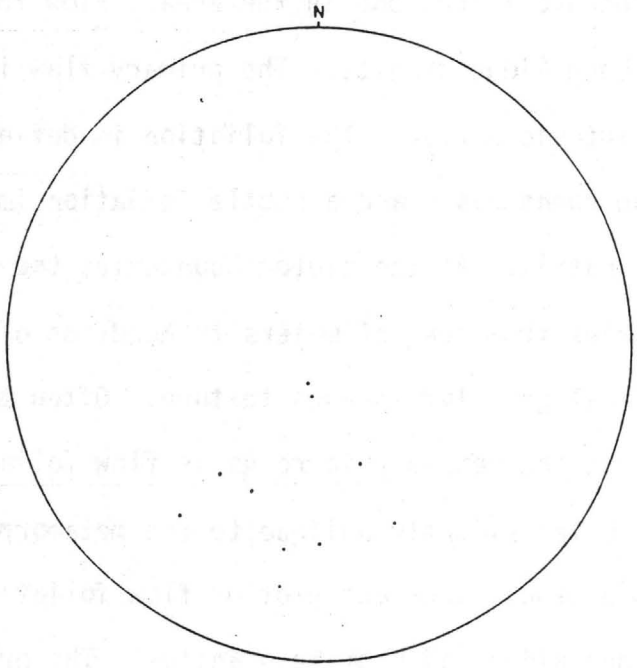

Figure 38. Plot of Pole to Primary Flow Foliations (P_1) on an Equal Area Net.

Imprinted on the Precambrian fabric are northwest trending faults of late Tertiary age.

Chapter 6

CHRONOLOGY OF EVENTS

Basite Accumulation

The oldest geologic event for which there is evidence in the Morgan Butte area is the accumulation of the original basites that were later metamorphosed to become amphibolites. The basites are probably contemporaneous with the accumulation of the Yavapai Series. It is unknown whether the basites were submarine accumulations of mafic lavas, subaerial accumulations, or intrusive sills. Blastoporphyritic textures suggest the original texture was that of phenocrysts in a fine-grained or aphanitic groundmass. Several other lines of evidence suggest the amphibolites were igneous in origin and not calcareous muds or dirty dolostones (See Chapter 1).

Premetamorphic Plutonism

Subsequent to the accumulation of the Yavapai Series and prior to the metamorphic episode that affected the Vishnu and Pinal Series, as well as the Yavapai Series, a plutonic intrusion of monzogranite invaded the area. Xenoliths and stoped blocks of the basites abounded in the granitic melt. There is scanty evidence that other types of country rock were present, interbedded with or intruded by the basites that did not survive the granitic intrusion (or the later metamorphism) as discrete xenoliths (See Origin of Granitic Gneiss). Exposures of the Yavapai Series in surrounding areas show a more heterogeneous and intricate

sequence of metamorphic rocks. Quartz-mica schists and quartzites in the White Picacho pegmatite area (Johns, 1952), and mica schists in the Castle Creek area (Ward, 1977) are not present in the Morgan Butte area. Presumably the rocks of highest melting temperature (i.e. basaltic composition) would be the last to be assimilated, if at all, particularly in a crystallizing melt of granitic composition.

Metamorphism

A major regional tectonic event metamorphosed the basites and monzogranite to the lower amphibolite facies. This event is correlative with the metamorphism and deformation dated at least at 1690 m.y. ago (Lanphere, 1968) that is prominent in the Yavapai Series in the Bradshaw Mountains. Mineralogic adjustment is more sensitive in metabasites than orthogneisses, and this allowed a metamorphic facies to be determined for both metamorphic rocks. A metamorphic fabric (S_1) is pervasive throughout both the amphibolites and granitic gneiss; however, the metamorphic effect upon the latter was primarily the development of the S_1 foliation. The metabasites at the lower amphibolite facies show an equilibrium assemblage of blue-green hornblende, andesine, plagioclase, epidote, and biotite.

Postmetamorphic Plutonism

Initiation of postmetamorphic plutonism apparently began with the intrusion of the small igneous bodies exposed in the southern parts of the area. The episode culminated in the emplacement of the batholithic biotite granite exposed in the northern parts of the area. Granitic dikes associated with the biotite granite intruding the hornblende diorite,

Black Rock granite and the hornblende biotite granodiorite are evidence the smaller plutons are older than the batholith. The biotite granite is similar to the Crazy Basin Quartz Monzonite dated at 1624 m.y. by Blacet (1968) in intrusive characteristics, composition, and the exceptional amount of tourmaline-bearing late stage fluids.

The Black Rock granite developed a mafic border of dioritic composition where it is in intrusive contact with one of the major bodies of amphibolite. The change in composition is clearly due to partial assimilation of amphibolite xenoliths. The hornblende biotite granodiorite exposed on the west side of the Black Rock granite is probably similar in origin to the mafic border phase on the east side. The granodiorite, however, was reintruded by the granite.

The intrusion of the biotite granite extended well beyond the thesis area (Figure 1). The intrusion has had a profound effect on these metamorphic rocks. The S_1 deformation in the form of small drag folds and kinks (F_1), as well as major warping is probably related to the forceful intrusion. Major warping includes the flexure on Morgan Butte and the change in strike of foliation along the batholith border. It is interesting to note that flow foliation readings from the various plutons are similar in orientation, and, in addition, are similar to the regional metamorphic foliation. This suggests that the various plutons are somewhat contemporaneous and intruded while the regional stresses that produced the metamorphic foliation were still in effect.

Injection of abundant granitic dikes, pegmatites, and medium grained granitic phases from the biotite granite, and their associated metasomatism, apparently initiated a retrograde metamorphism affecting the amphibolites and granitic gneiss. The retrograde alteration is not ubiquitous

throughout the metamorphic terrane, suggesting it was not a regional event. The retrograde alteration had several mineralogic effects. Chloritization of hornblende and biotite with development of more magnetite is common in both metamorphic rocks according to their respective mineralogies. Breakdown of andesine to produce albite, sericite, and epidote is typical in the amphibolites. Sericite and epidote are the typical products in the granitic gneiss. Similar alterations occur in the smaller plutonic bodies, but are difficult to distinguish from deuteric alteration.

The last intrusive event considered to be Precambrian is the emplacement of a hornblende diorite dike on the Red Bluff mine properties. The dike cuts through the biotite granite showing it to be younger than the batholith. An identical dike that is probably contemporaneous cuts through the granitic gneiss several hundred meters to the south. Both of these dikes are petrographically similar to the larger body of hornblende diorite to the south. Although a younger age cannot be ruled out, the dikes are considered as Precambrian because of this similarity. The hornblende diorite dikes differ from the Tertiary mafic dikes in that the dikes are entirely phaneritic.

Hiatus

There is a marked hiatus in the geologic record between the older Precambrian of Arizona and the late Cenozoic events in the Morgan Butte area. There are no remnants of the younger Precambrian or Paleozoic sediments that occur in other parts of central Arizona. It is unknown what kind of structural effects later tectonic events had on the rocks of the area. For example, the uplift in central Arizona that produced

the Mogollon Highlands in middle Triassic times (Wilson, 1962) involved the Morgan Butte area as part of the mountain region extending northwest and southeast through the state. What was the nature of the uplift and its effect upon the orientation of the rocks?

Late Cenozoic Events

The most recent tectonic event in the area is the development and formation of the Basin and Range Province. A northeast-southwest extensional stress regime resulted in the development of the Castle Hot Springs tectonovolcanic depression. The volcanics, considered to be Miocene (?) (Ward, 1977) are located in a northwest trending graben to which the Morgan Butte area is the westerly horst. The prominent northwest structural fabric (faulting, jointing) is also present in the horst and has profoundly controlled emplacement of rhyolite porphyry dikes, mafic dikes, and hydrothermal vein deposits.

The veins have been deposited from hydrothermal emanations from the volcanics or their underlying source. The fluids have severely altered both Precambrian and Tertiary rocks in zones up to 8 meters (26 ft.) on either side of the veins. The dikes are probably derived from a similar underlying source as the volcanics.

The last geologic event of significance is a supergene alteration of the veins by meteoric groundwaters. Oxidation, solution, and alteration is resulting in a conspicuous gossan where the veins are exposed at the surface. The nature of the alteration is to residually enrich the veins in gold above the water table and enrich them in copper below the water table. The supergene processes presumably have been an ongoing near surface event and are continuing at this moment.

REFERENCES CITED

Anderson, C. A., 1951, Older Precambrian structure in Arizona: Geol. Soc. Am. Bull., v. 62, p. 1331-1346.

Badgley, P. C., 1959, Structural methods for the exploration geologist: Harper and Brothers, Publishers, New York, N.Y., 280p.

Bastin, E. S., 1922, Primary native silver ores near Wickenburg, Arizona and their bearing on the genesis of the silver ores of Cobalt, Ontario: U.S. Geol. Surv. Bull. 735, p. 131-155.

Blacet, P. M., 1968, Precambrian geology of the southeast ¼ of the Mount Union quadrangle, Bradshaw Mountains, Central Arizona: unpublished Ph.D. dissertation, Stanford University, Calif., 244p.

Deer, W. A., Howie, R. A., and Zussman, J., 1964, Rock forming minerals: Vol. 1-5, John Wiley and Sons, Inc., New York, N.Y.

Higgins, M. W., 1971, Cataclastic rocks: Geological Survey Professional Paper 687, 97p.

Hyndman, D. W., 1972, Petrology of igneous and metamorphic rocks: McGraw-Hill Book Co., New York, N.Y., 533p.

Jaggar, T. A., Jr., and Palache, C., 1905, Description of Bradshaw Mountains quadrangle, Arizona: U.S. Geol. Surv. Geol. Atlas, folio 126, 11p.

Johns, R. H., 1952, Pegmatite deposits of the White Picacho District, Maricopa and Yavapai Counties, Arizona: Bureau of Geology and Mineral Technology Bulletin 162, University of Arizona, Tucson, 105p.

Keith, S. B., 1969, Map of known nonferrous base and precious metal mineral occurrences in Arizona: Map 4-1, Bureau of Geology and Mineral Technology, University of Arizona, Tucson.

Lanphene, M. A., 1968, Geochronology of the Yavapai Series of Central Arizona: Canadian Journal of Earth Sciences, vol. 5, pp. 757-762.

Lindgren, W., 1926, Ore deposits of the Jerome and Bradshaw Mountains quadrangles, Arizona: U.S. Geol. Surv. Bull. 782, 192p.

Livingston, D. E., and Damon, P. E., 1968, The age of stratified Precambrian rock sequences in Central Arizona and Northern Sonora: Canadian Journal of Earth Sciences, vol. 5, pp. 763-772.

London, D., 1979, Occurrence and alteration of lithium minerals, White Picacho pegmatites: unpublished M.S. thesis, Arizona State University, Tempe, 131p.

McBirney, A. R., 1979, Effects of assimilation in Evolution of the Igneous Rocks Fiftieth Anniversary Perspectives, H. S. Yoder, Jr., ed., Princeton University Press, Princeton, New Jersey, 588p.

Miyashiro, A., 1973, Metamorphism and metamorphic belts: John Wiley and Sons, Inc., New York, N.Y., 492p.

Moorehouse, W. W., 1959, The study of rocks in thin section: Harper and Row, Publishers, New York and Evanston, 514p.

Park, C. F., Jr., and MacDiarmid, R. A., 1975, Ore deposits: 3rd Ed. W. H. Freeman and Company, San Francisco, Calif., 530p.

Pierce, H. W., Keith, S. B., and Wilt, C. W., 1970, Coal, oil, natural gas, helium, and uranium in Arizona: Bureau of Geology and Mineral Technology Bulletin 182, University of Arizona, Tucson, 289p.

Robinson, P., and Jaffe, H. W., 1969, Chemographic exploration of amphibolite assemblages from Central Massachusetts and Southwestern New Hampshire in Mineral. Soc. Amer. Spec. Pap. 2, pp. 251-274.

Streckeisen, A., 1976, To each plutonic rock its' proper name: Earth Science Review, v. 12, p. 1-33.

Vrba, S. L., 1980, Precambrian geology of the Cleator area, Yavapai County, Arizona: unpublished M.S. thesis, Northern Arizona University, 96p.

Ward, M. B., 1977, The volcanic geology of the Castle Hot Springs area, Yavapai County, Arizona: unpublished M.S. thesis, Arizona State University, Tempe, 74p.

Wilson, E. D., 1962, A resume of the geology of Arizona: Bureau of Geology and Mineral Technology Bulletin 171, University of Arizona, Tucson, 140p.

APPENDIX I

Calculated Chemical Analyses

APPENDIX I

Calculated Chemical Analyses

A technique of calculating whole rock oxide weight percents is outlined here, as this thesis relies heavily on the results. The technique departs from using ideal stoichiometric mineral compositions, and instead uses real mineral oxide weight percent analyses as standards to more accurately approximate reality. The real mineral analyses used as standards in the calculation were chosen from geologic situations as similar as possible to those in the Morgan Butte area.

The technique is intended to be the best possible alternative in the absence of detailed expensive laboratory chemical analyses. Unfortunately, the technique can be applied only to coarser grained rocks from which point count studies can be taken. Fortunately, coarse-grained rocks is the rule in the Morgan Butte area.

I. Normally, an ideal oxide weight percent for each mineral represented in the rock would be the first step in such a calculation. The results for each mineral would be tabulated for later use in calculating total rock oxide weight percents for each oxide. The ideal approach would use the following equations:

$$\text{Wt\% of oxide in mineral} = \frac{\text{mol. wt. of oxide}}{\text{mol. wt. of mineral}}$$

where:

mol. wt. of oxide = mol. wt. of cation and mol. wt. of oxygen by stoichiometric number(s)

and:

mol. wt. of mineral = mol. wt. of each element by stoichiometric number(s)

Instead, the real mineral oxide weight percents are used. This increases the accuracy of the calculation by taking into account impurities and amounts of elements not included in the ideal mineral formula. For example, the albite used was from an amphibolite in Italy and contains small amounts of K_2O, H_2O^+, CaO, Fe_2O_3 and MgO that would be missed in the ideal approach. Several different analyses of plagioclase were used to represent differing compositions and occurrences of plagioclase.

II. Accurate modal percents (corrected for alteration) of mineral compositions of each rock taken from point counts are then corrected for density variations. This eliminates possible inaccuracy by treating the rock as uniformly dense. The equation for this correction is as follows:

$$\text{Modal \% corrected for density} = \frac{\text{Modal \% x density}}{\text{Modal \% of each mineral x density}}$$

Multiply (and tabulate) the modal percent for each mineral by its density and summate beforehand, as this will allow the process to be done quickly and efficiently.

III. To arrive at a total oxide weight percent for each rock, multiply the oxide weight proportion in each mineral by the corrected modal percent of each mineral, and sum. This collects the oxide weight percent contribution from each mineral in the rock for that particular oxide. This is done for each oxide in each mineral to arrive at a simulated whole rock analysis. The equation for this part of the procedure is as follows:

$$\text{wt \% of oxide in rock} = \frac{\text{wt \% of oxide in each mineral}}{100} \times \text{modal \% (corrected) of each mineral}$$

The most efficient way to proceed is to tabulate the oxide weight percent breakdown for each mineral used as a standard on a separate sheet, along with their respective densities. The calculation for each rock sample is done on separate sheets, for which the mineral standard is used for reference.

Mineral	SiO_2	TiO_2	Al_2O_3	Fe_2O_3	FeO	MnO	MgO	CaO	Na_2O	K_2O	H_2O+	H_2O-	P_2O_5	F	D
Hornblende	44.64	.97	9.95	4.94	17.25	.23	8.57	9.45	1.549	.31	2.30	.37	.01	.01	3.246
Plagioclase An35-40	58.1	-	26.44	.04	.15	-	.03	7.84	6.48	1.1	.03	.06	-	-	2.652
Plagioclase An 20	64.1	-	22.66	.14	.17	-	.25	3.26	9.89	.05	.17	.06	-	-	2.646
Albite	67.41	-	20.5	.07	-	-	.1	.81	10.97	.36	.15	-	-	-	2.619
Microcline	64.2	-	19.1	.4	-	-	-	.34	2.60	12.76	.72	-	-	-	2.577
Orthoclase	64.76	-	19.96	.08	-	-	-	.84	5.54	8.12	.54	-	-	-	2.595
Biotite	37.17	3.14	14.6	3.75	26.85	.06	4.23	.17	.15	8.25	1.35	-	-	.85	2.925
Muscovite	48.42	.87	27.16	6.57	.81	-	-	-	.35	11.23	4.31	.19	-	-	2.88
Chlorite	25.62	.88	21.19	3.88	21.55	.35	15.78	.16	-	-	10.87	.19	-	-	2.75
Quartz	100	-	-	-	-	-	-	-	-	-	-	-	-	-	2.625
Epidote	36.92	-	22.25	15.21	.57	.75	-	23.11	-	-	1.16	.16	-	-	3.43
Sphene	30.35	35.44	2.15	2.5	-	.25	.1	26.46	-	.02	.93	.17	-	.67	3.54
Apatite	-	-	-	-	-	.07	.1	55.84	-	-	1.86	-	42.05	.16	3.21
Magnetite	.48	2.98	.02	63.4	32.25	-	.39	.23	-	-	-	-	-	-	5.18
Ilmenite	.14	49.89	.02	6.26	40.39	.41	2.27	.34	-	-	.06	-	-	-	4.7

Mineral	Modal %	Modal % correct	SiO_2	TiO_2	Al_2O_3	Fe_2O_3	FeO	MnO	MgO	CaO	Na_2O	K_2O	H_2O+	H_2O-	P_2O_5	F
Hornblende																
Andesine	18.5	18.078	10503	0	4.780	.007	.027	0	.005	1.417	1.171	.199	.005	.011	0	0
Oligoclase																
Albite																
Microcline	24.0	22.790	14631	0	4.353	.091	0	0	0	.077	.592	2.908	.164	0	0	0
Orthoclase																
Biotite																
Muscovite	22.5	23.877	11561	.208	6.485	1.569	.193	0	0	0	.083	2.681	1.029	.045	0	0
Chlorite	10.0	10.133	2.596	.089	2.147	.393	2.184	.035	1.599	.016	0	0	1.101	.019	0	0
Quartz	24.0	23.214	23214	0	0	0	0	0	0	0	0	0	0	0	0	0
Epidote																
Sphene																
Apatite																
Magnetite	1.0	1.909	.009	.057	0	1.210	.616	0	.007	.004	0	0	0	0	0	0
			62505	.354	17765	3.270	3.02	.035	1.611	1.514	1.846	5.788	2.299	.075	0	0

PCmvMB: 100.082%

Mineral	Modal %	Modal % correct	SiO_2	TiO_2	Al_2O_3	Fe_2O_3	FeO	MnO	MgO	CaO	Na_2O	K_2O	H_2O+	H_2O-	P_2O_5	F
Hornblende																
Andesine	26.52	25.855	15022	0	6.836	.010	.039	0	.088	2.027	1.675	.284	.008	.015	0	0
Oligoclase																
Albite																
Microcline	22.0	20.842	13380	0	3.981	.083	0	0	0	.071	.542	2.659	.150	0	0	0
Orthoclase																
Biotite	7.52	8.086	3.005	.254	1.180	.303	2.171	.005	.342	.014	.012	.667	.109	0	0	.069
Muscovite	7.48	7.919	3.834	.069	2.151	.520	.064	0	0	0	.028	.889	.341	.015	0	0
Chlorite	.48	.485	.124	.004	.103	.019	.104	.002	.076	.001	0	0	.053	.001	0	0
Quartz	29.0	27.985	27985	0	0	0	0	0	0	0	0	0	0	0	0	0
Epidote	7.0	8.826	3.258	0	1.964	1.342	.050	.066	0	2.040	0	0	.102	.014	0	0
Sphene																
Apatite																
Magnetite																
			66608	.327	16215	2.277	2.428	.073	.426	4.153	2.257	4.499	.763	.045	0	.069
			66515	.326	16192	2.274	2.425	.073	.425	4.147	2.254	4.493	.762	.045	0	.069

PCmv7: 100.140 or 100.00(corrected)%

Mineral	Modal %	Modal % correct	SiO_2	TiO_2	Al_2O_3	Fe_2O_3	FeO	MnO	MgO	CaO	Na_2O	K_2O	H_2O+	H_2O-	P_2O_5	F
Hornblende	10.0	11.38	5.080	.110	1.132	.562	1.963	.026	.975	1.075	.176	.035	.262	.042	.001	.001
Andesine	20.0	18.59	10800	0	4.915	.007	.027	0	.056	1.457	1.205	.204	.005	.011	0	0
Oligoclase																
Albite																
Microcline																
Orthoclase																
Biotite	40.0	41.01	15243	1.287	5.987	1.537	11011	.025	1.734	.070	.061	3.383	.553	0	0	.350
Muscovite																
Chlorite																
Quartz	25.0	23.01	23.01	0	0	0	0	0	0	0	0	0	0	0	0	0
Epidote	5.0	6.01	2.218	0	1.337	.914	.034	.045	0	1.390	0	0	.070	.009	0	0
Sphene																
Apatite																
Magnetite																
			56351	1.397	13370	3.020	13035	.096	2.765	3.990	1.442	3.622	.890	.062	.001	.351

PCmv9: 100.392%

Mineral	Modal %	Modal % correct	SiO_2	TiO_2	Al_2O_3	Fe_2O_3	FeO	MnO	MgO	CaO	Na_2O	K_2O	H_2O+	H_2O-	P_2O_5	F
Hornblende																
Andesine	34.04	33.598	19520	0	8.883	.013	.050	0	.010	2.634	2.177	.369	.010	.020	0	0
Oligoclase																
Albite																
Microcline	32.0	30.692	19704	0	5.862	.123	0	0	0	.104	.798	3.916	.221	0	0	0
Orthoclase																
Biotite	11.4	12.410	4.613	.390	1.812	.465	3.332	.007	.525	.021	.019	1.024	.167	0	0	.105
Muscovite	2.96	3.173	1.536	.028	.862	.208	.026	0	0	0	.011	.356	.137	.006	0	0
Chlorite	.6	.614	.157	.005	.130	.024	.132	.002	.097	.001	0	0	.067	.001	0	0
Quartz	18.0	17.585	17585	0	0	0	0	0	0	0	0	0	0	0	0	0
Epidote																
Sphene																
Apatite																
Magnetite	1.0	1.928	.009	.057	0	1.222	.622	0	.007	.004	0	0	0	0	0	0
			63115	.480	17549	2.055	4.162	.009	.639	2.764	3.005	5.665	.602	.027	0	.105

PCmv17: 100.177 %

Mineral	Modal %	Modal % correct	SiO_2	TiO_2	Al_2O_3	Fe_2O_3	FeO	MnO	MgO	CaO	Na_2O	K_2O	H_2O+	H_2O-	P_2O_5	F
Hornblende	61.0	63.431	28315	.615	6.311	3.133	10942	.146	5.436	3.749	.982	.197	1.459	.235	.006	.006
Andesine	31.5	26.761	18301	0	7.076	.011	.040	0	.008	2.098	1.734	.006	.008	.016	0	0
Oligoclase																
Albite	.70	.587	.396	0	.120	0	0	0	0	.005	.064	.002	.001	0	0	0
Microcline																
Orthoclase																
Biotite																
Muscovite	2.80	2.583	1.251	.022	.701	.170	.021	0	0	0	.009	.290	.111	.005	0	0
Chlorite																
Quartz																
Epidote																
Sphene																
Apatite																
Magnetite	4.0	6.638	.032	.198	.001	4.208	2.141	0	.026	.015	0	0	0	0	0	0
			48295	.835	14209	7.522	13144	.146	5.470	5.867	2.789	.495	1.579	.256	.006	.006

PCmv36: 100.619%

Mineral	Modal %	Modal % correct	SiO_2	TiO_2	Al_2O_3	Fe_2O_3	FeO	MnO	MgO	CaO	Na_2O	K_2O	H_2O+	H_2O-	P_2O_5	F
Hornblende																
Andesine																
Oligoclase																
Albite																
Microcline																
Orthoclase																
Biotite																
Muscovite	16.5	14.741	7.137	.128	4.004	.968	.119	0	0	0	.051	1.655	.635	.028	0	0
Chlorite	49.5	42.228	12605	.372	8.948	1.638	9.10	.148	6.663	.067	0	0	4.590	.080	.0	0
Quartz	22.0	17.915	17915	0	0	0	0	0	0	0	0	0	0	0	0	0
Epidote																
Sphene																
Apatite																
Magnetite	12.0	19.283	.092	.575	.004	12225	6.219	0	.075	.044	0	0	0	0	0	0
Ilmenite	4.0	5.832	.008	2.909	.001	.365	2.355	.024	.132	.020	0	0	.003	0	0	0
			37757	3.984	12957	15190	17793	.172	6.870	.131	.051	1.655	5.228	.108	0	0
			37052	3.910	12715	14912	17461	.169	6.742	.128	.050	1.624	5.130	.105	0	0

PCmv38: 101.902 or 99.998(corrected)%

Mineral	Modal %	Modal % correct	SiO_2	TiO_2	Al_2O_3	Fe_2O_3	FeO	MnO	MgO	CaO	Na_2O	K_2O	H_2O+	H_2O-	P_2O_5	F
Hornblende	44.0	48.056	21452	.466	4.781	2.374	8.290	.110	4.118	4.541	.744	.149	1.105	.178	.005	.005
Andesine	50.35	44.930	26104	0	11879	.018	.067	0	.013	3.522	2.911	.494	.013	.027	0	0
Oligoclase																
Albite	2.65	2.335	1.574	0	.479	.002	0	0	0	.019	.256	.008	.003	0	0	0
Microcline																
Orthoclase																
Biotite																
Muscovite																
Chlorite																
Quartz																
Epidote																
Sphene	1.0	1.191	.361	.422	.026	.030	0	.003	0	.315	0	0	.011	.002	0	.008
Apatite																
Magnetite	2.0	3.486	.017	.104	.001	2.210	1.124	0	.013	.008	0	0	0	0	0	0
			49508	.992	17166	4.634	9.481	.113	4.144	8.405	3.911	.651	1.132	.207	.005	.013

PCmv39: 100.362 %

Mineral	Modal %	Modal % correct	SiO_2	TiO_2	Al_2O_3	Fe_2O_3	FeO	MnO	MgO	CaO	Na_2O	K_2O	H_2O+	H_2O-	P_2O_5	F
Hornblende																
Andesine	30.4	30.402	12663	0	8.038	.012	.046	0	.009	2.383	1.970	.334	.009	.018	0	0
Oligoclase																
Albite																
Microcline	35.0	34.013	21836	0	6.496	.136	0	0	0	.116	.884	4.340	.245	0	0	0
Orthoclase																
Biotite	8.55	9.431	3.505	.296	1.377	.354	2.532	.006	.399	.016	.014	.778	.127	0	0	.080
Muscovite	3.60	3.910	1.893	.034	1.062	.257	.032	0	0	0	.014	.439	.168	.007	0	0
Chlorite	.45	.466	.119	.004	5.429	.018	.10	.002	.073	.001	0	0	.051	.001	0	0
Quartz	22.0	21.178	21178	0	0	0	0	0	0	0	0	0	0	0	0	0
Epidote																
Sphene																
Apatite																
Magnetite																
			66194	.334	22402	.777	2.710	.008	.481	2.516	2.882	5.891	.60	.026	0	.080
			63101	.318	21355	.741	2.583	.008	.458	2.398	2.747	5.616	.572	.025	0	.076

FPCmv7: 104.901 or 99.998(corrected) %

Mineral	Modal %	Modal % correct	SiO_2	TiO_2	Al_2O_3	Fe_2O_3	FeO	MnO	MgO	CaO	Na_2O	K_2O	H_2O+	H_2O-	P_2O_5	F
Hornblende	59.0	61.411	27.413	.596	6.110	3.034	10.593	.141	5.263	5.803	.951	.190	1.412	.227	.006	.006
Andesine																
Oligoclase																
Albite																
Microcline	5.0	4.132	2.653	0	.789	.016	0	0	0	.014	.107	.527	.030	0	0	0
Orthoclase																
Biotite																
Muscovite	25.0	23.088	11.179	.201	6.271	1.517	.187	0	0	0	.081	2.593	.995	.044	0	0
Chlorite																
Quartz	5.0	4.209	4.209	0	0	0	0	0	0	0	0	0	0	0	0	0
Epidote	5.0	5.499	2.030	0	1.223	.836	.031	.041	0	1.271	0	0	.064	.009	0	0
Sphene																
Apatite																
Magnetite	1.0	1.661	.008	.049	0	1.053	.536	0	.006	.004	0	0	0	0	0	0
			47.492	.846	14.393	6.456	11.347	.182	5.269	7.092	1.139	3.310	2.501	.280	.006	.006

FPCmv17: 100.319%

Mineral	Modal %	Modal % correct	SiO_2	TiO_2	Al_2O_3	Fe_2O_3	FeO	MnO	MgO	CaO	Na_2O	K_2O	H_2O+	H_2O-	P_2O_5	F
Hornblende																
Andesine	29.44	29.406	17085	0	7.775	.041	.044	0	.009	2.305	1.905	.323	.009	.018	0	0
Oligoclase																
Albite																
Microcline	28.0	27.178	17448	0	5.191	1.785	0	0	0	.092	.707	3.468	.196	0	0	0
Orthoclase																
Biotite	6.50	7.161	2.662	.225	1.045	.268	1.923	.004	.303	.012	.011	.591	.097	0	0	.061
Muscovite	4.56	4.946	2.395	.043	1.343	.325	.040	0	0	0	.017	.555	.213	.009	0	0
Chlorite	3.50	3.625	.929	.032	.768	.141	.781	.013	.572	.006	0	0	.394	.007	0	0
Quartz	28.0	27.683	27683	0	0	0	0	0	0	0	0	0	0	0	0	0
Epidote																
Sphene																
Apatite																
Magnetite																
			68202	.300	16122	2.560	2.788	.017	.884	2.415	2.640	4.937	.909	.034	0	.061
			66951	.294	15826	2.513	2.737	.017	.868	2.371	2.591	4.846	.892	.033	0	.060

PPCmv18: 101.869 or 99.999(corrected)%

Mineral	Modal %	Modal % correct	SiO_2	TiO_2	Al_2O_3	Fe_2O_3	FeO	MnO	MgO	CaO	Na_2O	K_2O	H_2O+	H_2O-	P_2O_5	F
Hornblende	53.9	57.508	25671	.558	5.722	2.841	9.920	.132	4.928	5.434	.891	.178	1.323	.213	.006	.006
Andesine	18.04	15.725	9.136	0	4.158	.006	.023	0	.005	1.233	1.019	.173	.005	.009	0	0
Oligoclase																
Albite	1.10	.947	.638	0	.194	.001	0	0	0	.008	.104	.003	.001	0	0	0
Microcline																
Orthoclase																
Biotite																
Muscovite	3.96	3.749	1.815	.033	1.018	.246	.030	0	0	0	.013	.421	.161	.007	0	0
Chlorite																
Quartz	15.0	12.942	12942	0	0	0	0	0	0	0	0	0	0	0	0	0
Epidote	5.0	5.637	2.081	0	1.254	.857	.032	.042	0	1.303	0	0	.065	.009	0	0
Sphene	3.0	3.491	1.050	1.237	.075	.087	0	.009	0	.924	0	.001	.032	.006	0	.023
Apatite																
Magnetite																
			51333	1.828	12421	4.038	10005	.183	4.933	8.902	2.027	.776	1.587	.244	.006	.029

FPCmv20: 100.304 %

Mineral	Modal %	Modal % correct	SiO_2	TiO_2	Al_2O_3	Fe_2O_3	FeO	MnO	MgO	CaO	Na_2O	K_2O	H_2O+	H_2O-	P_2O_5	F
Hornblende	15.327	16.169	7.218	.157	1.609	.799	2.789	.037	1.386	1.528	.250	.050	.372	.060	.002	.002
Andesine																
Oligoclase																
Albite	.313	.266	.179	0	.054	0	0	0	0	.002	.029	.001	0	0	0	0
Microcline																
Orthoclase																
Biotite	15.64	14.868	5.526	.467	2.171	.557	3.992	.009	.629	.025	.022	1.227	.201	0	0	.126
Muscovite	20.0	18.720	9.064	.163	5.084	1.230	.152	0	0	0	.065	2.102	.807	.035	0	0
Chlorite	2.72	2.431	.623	.021	.515	.094	.524	.008	.384	.004	0	0	.264	.005	0	0
Quartz	28.0	23.888	23888	0	0	0	0	0	0	0	0	0	0	0	0	0
Epidote	7.0	7.803	2.881	0	1.736	1.187	.044	.058	0	1.803	0	0	.090	.012	0	0
Sphene	5.0	5.752	1.746	2.038	.123	.144	0	.014	.006	1.522	0	.001	.053	.010	0	.038
Apatite																
Magnetite	6.0	10.101	.048	.301	.002	.632	3.257	0	.039	.023	0	0	0	0	0	0
			51173	3.147	11294	4.643	10758	.126	2.444	4.907	.366	3.381	1.787	.122	.002	.166
			54257	3.337	11975	4.923	11406	.133	2.591	5.203	.388	3.585	1.895	.129	.002	.176

FPCmv21: 94.316 or 100.00(corrected)%

Mineral	Modal %	Modal % correct	SiO_2	TiO_2	Al_2O_3	Fe_2O_3	FeO	MnO	MgO	CaO	Na_2O	K_2O	H_2O+	H_2O-	P_2O_5	F
Hornblende	52.0	55.186	24635	.535	5.491	2.726	9.519	.127	4.729	5.215	.855	.171	1.269	.204	.005	.005
Andesine	17.2	14.913	8.664	0	3.943	.006	.022	0	.004	1.169	.966	.164	.004	.009	0	0
Oligoclase																
Albite																
Microcline																
Orthoclase																
Biotite																
Muscovite	25.8	24.293	11763	.211	6.598	1.596	.197	0	0	0	.085	2.728	1.047	.046	0	0
Chlorite																
Quartz																
Epidote	5.0	5.607	2.070	0	1.247	.853	.032	.042	0	1.296	0	0	.065	.009	0	0
Sphene																
Apatite																
Magnetite																
			47132	.746	17279	5.181	9.77	.169	4.733	7.68	1.906	3.063	2.385	.268	.005	.005

PPCmv23: 100.322%

Mineral	Modal %	Modal % correct	SiO_2	TiO_2	Al_2O_3	Fe_2O_3	FeO	MnO	MgO	CaO	Na_2O	K_2O	H_2O+	H_2O-	P_2O_5	F
Hornblende	44.1	48.477	21.640	.470	4.823	2.395	8.362	.111	4.154	4.581	.751	.150	1.115	.179	.005	.005
Andesine	35.0	31.433	18.262	0	8.311	.012	.047	0	.009	2.464	2.037	.346	.009	.019	0	0
Oligoclase																
Albite	.90	.798	.538	0	.163	0	0	0	0	.006	.087	.003	.001	0	0	0
Microcline																
Orthoclase																
Biotite																
Muscovite																
Chlorite																
Quartz	15.0	13.334	13334	0	0	0	0	0	0	0	0	0	0	0	0	0
Epidote	1.0	1.161	.429	0	.258	.176	.007	.009	0	.268	0	0	.013	.002	0	0
Sphene	4.0	4.795	1.455	1.699	.103	.120	0	.012	.005	1.269	0	.001	.044	.008	0	.032
Apatite																
Magnetite																
			55658	2.169	13658	2.703	8.416	.132	4.168	8.588	2.875	.500	1.182	.208	.005	.037

FPCmv29: 100.299 %

Mineral	Modal %	Modal % correct	SiO_2	TiO_2	Al_2O_3	Fe_2O_3	FeO	MnO	MgO	CaO	Na_2O	K_2O	H_2O+	H_2O-	P_2O_5	F
Hornblende	72.0	73.205	32679	.710	7.284	3.616	12628	.168	6.274	6.918	1.134	.227	1.684	.271	.007	.007
Andesine																
Oligoclase																
Albite																
Microcline																
Orthoclase																
Biotite	7.68	7.036	2.615	.221	1.027	.264	1.889	.004	.298	.012	.010	.580	.095	0	0	.060
Muscovite	18.0	16.238	7.862	.141	4.410	1.067	.131	0	0	0	.057	1.823	.70	.031	0	0
Chlorite	.32	.276	.071	.002	.058	.011	.059	.001	.043	0	0	0	.030	0	0	0
Quartz																
Epidote																
Sphene																
Apatite																
Magnetite	2.0	3.245	.015	.097	.001	2.057	1.046	0	.013	.007	0	0	0	0	0	0
			43242	1.171	12780	7.015	15753	.173	6.628	6.937	1.201	2.630	2.509	.302	.007	.067

PPCmv36: 100.415 %

Mineral	Modal %	Modal % correct	SiO_2	TiO_2	Al_2O_3	Fe_2O_3	FeO	MnO	MgO	CaO	Na_2O	K_2O	H_2O+	H_2O-	P_2O_5	F
Hornblende	57.0	59.670	26637	.579	5.937	2.948	10293	.137	5.114	5.639	.924	.185	1.372	.221	.006	.006
Andesine	27.88	23.845	13854	0	6.305	.009	.036	0	.007	1.869	1.545	.262	.007	.014	0	0
Oligoclase																
Albite	1.36	1.149	.774	0	.235	.001	0	0	0	.009	.126	.004	.002	0	0	0
Microcline																
Orthoclase																
Biotite																
Muscovite	4.76	4.421	2.141	.038	1.201	.290	.036	0	0	0	.015	.496	.190	.008	0	0
Chlorite																
Quartz	5.0	4.233	4.233	0	0	0	0	0	0	0	0	0	0	0	0	0
Epidote																
Sphene																
Apatite																
Magnetite	4.0	6.682	.032	.199	.001	4.236	2.155	0	.026	.015	0	0	0	0	0	0
			47671	.816	13679	7.484	12520	.137	5.147	7.532	2.610	.947	1.571	1.814	.006	.006

PPCmv37: 101.940 %

Mineral	Modal %	Modal % correct	SiO_2	TiO_2	Al_2O_3	Fe_2O_3	FeO	MnO	MgO	CaO	Na_2O	K_2O	H_2O+	H_2O-	P_2O_5	F
Hornblende	49.0	52.262	23330	.507	5.200	2.582	9.015	.120	4.479	4.939	.809	.162	1.202	.193	.005	.005
Andesine	44.65	38.908	22605	0	10287	.015	.058	0	.012	3.050	2.521	.428	.012	.023	0	0
Oligoclase																
Albite	2.35	2.022	1.363	0	.414	.001	0	0	.002	.016	.222	.007	.003	0	0	0
Microcline																
Orthoclase																
Biotite																
Muscovite																
Chlorite																
Quartz																
Epidote																
Sphene																
Apatite																
Magnetite	4.0	6.808	.033	.203	.001	.426	2.195	0	.026	.016	0	0	0	0	0	0
			47331	.710	15.902	3.024	11268	.120	4.519	8.021	3.552	.597	1.217	.216	.005	.005
			49.054	.736	16481	3.134	11678	.124	4.683	8.313	3.681	.619	1.261	.224	.005	.005

FPCmv39: 96.487 or 99.998(corrected)%

Mineral	Modal %	Modal % correct	SiO_2	TiO_2	Al_2O_3	Fe_2O_3	FeO	MnO	MgO	CaO	Na_2O	K_2O	H_2O+	H_2O-	P_2O_5	F
Hornblende	24.0	25.960	11588	.252	2.583	1.282	4.478	.060	2.225	2.453	.402	.080	.597	.096	.002	.002
Andesine	25.8	22.800	13247	0	6.028	.009	.034	0	.007	1.787	1.477	.251	.014	.014	0	0
Oligoclase																
Albite	1.20	1.047	.706	0	.215	.001	0	0	.001	.008	.115	.004	.001	0	0	0
Microcline																
Orthoclase																
Biotite	12.0	11.696	4.347	.367	1.708	.439	3.140	.007	.495	.020	.017	.965	.158	0	0	.099
Muscovite	3.0	2.879	1.394	.025	.782	.189	.023	0	0	0	.010	.323	.124	.005	0	0
Chlorite	4.0	3.665	.939	.032	.777	.142	.790	.013	.578	.006	0	0	.398	.007	0	0
Quartz	20.0	17.495	17495	0	0	0	0	0	0	0	0	0	0	0	0	0
Epidote	2.0	2.286	.844	0	.509	.348	.013	.017	0	.528	0	0	.026	.004	0	0
Sphene	3.0	3.539	1.074	1.254	.076	.088	0	.009	.003	.936	0	.001	.033	.006	0	.024
Apatite																
Magnetite	5.0	8.631	.041	.257	.002	5.472	2.783	0	.034	.020	0	0	0	0	0	0
			51675	2.187	12680	7.970	11261	.106	3.343	5.758	2.021	1.624	1.351	.132	.002	.125

FPCmv40: 100.235 %